Review

Lin Huang, Yusheng Zhang and Xueming Liu*

Dynamics of carbon nanotube-based mode-locking fiber lasers

https://doi.org/10.1515/nanoph-2020-0269
Received May 6, 2020; accepted June 2, 2020

Abstract: Carbon nanotube (CNT) can work as excellent saturable absorber (SA) due to its advantages of fast recovery, low saturation intensity, polarization insensitivity, deep modulation depth, broad operation bandwidth, outstanding environmental stability, and affordable fabrication. Its successful application as SA has promoted the development of scientific research and practical application of mode-locked fiber lasers. Besides, mode-locked fiber laser constitutes an ideal platform for investigating soliton dynamics which exhibit profound nonlinear optical dynamics and excitation ubiquitous in many fields. Up to now, a variety of soliton dynamics have been observed. Among these researches, CNT-SA is a key component that suppresses the environmental perturbation and optimizes the laser system to reveal the true highly stochastic and non-repetitive unstable phenomena of the initial self-starting lasing process. This review is intended to provide an up-to-date introduction to the development of CNT-SA based ultrafast fiber lasers, with emphasis on recent progress in real-time buildup dynamics of solitons in CNT-SA mode-locked fiber lasers. It is anticipated that study of dynamics of solitons can not only further reveal the physical nature of solitons, but also optimize the performance of ultrafast fiber lasers and eventually expand their applications in different fields.

Keywords: carbon nanotube; dispersive Fourier transform; fiber laser.

1 Introduction

Ultrafast pulses maintain significant applications in various fields, such as ultrafast imaging, optical communications, spectroscopy, biomedicine, and material processing. Passively mode-locked fiber lasers, which have been widely utilized to generate ultrashort pulses in the femtosecond level, can be regarded as the next-generation laser source that can replace the solid-state laser due to the advantages of high beam quality, high efficiency, high integration, high reliability, etc. [1]. For the passively mode-locked fiber lasers, saturable absorber (SA) plays a key role in generating ultrafast pulses. It works by depressing the transmissivity of pulses with low intensity while raising the transmissivity of pulses with high intensity. At present, common passive mode-locker in fiber lasers can be divided into effective and real SAs. The effective SAs, i. e., the nonlinear polarization rotation (NPR) [2] and nonlinear optical loop mirror (NOLM) [3], are based on nonlinear effect with the properties of high damage threshold and low cost, which provide a good platform for the research of nonlinear phenomena. However, due to their drawbacks including high saturation threshold, difficulty of self-starting and vulnerable to environmental perturbation, it is limited for practical applications. The real SAs, such as semiconductor saturable absorption mirror (SESAM) [4], are based saturation effect of resonance transition of the material. In fact, most light-absorbing materials can be used as the SA providing the laser operating in the material resonant absorption wavelength range. For the real SA, there are several parameters that are crucial for the performance of SA, including operating wavelength, saturable intensity, recovery time, damage threshold and thermal stability, etc. In recent years, SESAM is a leading passive mode-locked technology in commercial applications. It is mainly due to its mature fabrication process, which can control the process of fabricating SESAM, realize mode-locked devices with

Lin Huang and Yusheng Zhang: These authors contributed equally to this work.

***Corresponding author: Xueming Liu**, College of Astronautics, Nanjing University of Aeronautics and Astronautics, Nanjing 210016, China; State Key Laboratory of Modern Optical Instrumentation, College of Optical Science and Engineering, Zhejiang University, Hangzhou 310027, China, E-mail: liuxueming72@yahoo.com. https://orcid.org/0000-0001-5445-7178
Lin Huang: College of Astronautics, Nanjing University of Aeronautics and Astronautics, Nanjing 210016, China. https://orcid.org/0000-0002-8310-8644
Yusheng Zhang: College of Astronautics, Nanjing University of Aeronautics and Astronautics, Nanjing 210016, China

different characteristics, and meet various requirement [5, 6]. However, the SEASAM still faces several drawbacks, such as the expensive and complex preparation process, narrow operating wavelength range [5], slow recovery time, and poor compatibility with fibers. Therefore, researchers hope to find an ideal passive mode-locker with the features of fast response time, strong nonlinear effect, wide operating bandwidth, low unsaturated absorption loss, high damage threshold power, appropriate modulation depth, low cost, simple preparation method and appropriate integrated structure [7].

In recent years, various kinds of nanomaterials, such as carbon nanotubes (CNTs) [8–12], graphene [11, 13], transition metal chalcogenide (TMD) [14], black phosphorus [15], and topological insulator [16], etc., show up semiconductor characteristics of strong third-order nonlinear effect, ultrafast response time and wide band operating wavelength range, thereby can be applied as competitive real SA. In particular, CNT-SA has been widely studied and applied in mode-locked fiber lasers by taking advantages of fast recovery, low saturation intensity, polarization insensitivity, deep modulation depth, broad operation bandwidth, outstanding environmental stability, and affordable fabrication. Its successful application as SA has promoted the development scientific research of mode-locked fiber lasers and has become the building block of the advances of mode-locked fiber lasers.

On the other hand, ultrafast mode-locking fiber lasers can provide an excellent platform for observing a variety of nonlinear dynamics, such as modulation instability, Four-wave mixing, cross-phase modulation and so on [17]. Although some steady state phenomena had been observed theoretically and experimentally, many interesting and important transient dynamics properties of these nonlinear dynamics can only be theoretically predicted, and some are unpredictable. The main reason is that these ultrafast nonlinear dynamics are unrepeatable and have complex transformation in temporal and spectral domain, which cannot be resolved by the current technologies. In recent years, researchers have proposed time-stretched dispersive Fourier transform (TS-DFT) technique to measure the transient, non-repeat events [18–20]. The TS-DFT technique derives from the analogy between spatial Fraunhofer diffraction and temporal dispersion, in which the diffraction of a beam through a lens in the far-field region is analogous to the propagation of a time pulse in a dispersion element, also known as the space-time duality [21]. Up to now, a variety of soliton dynamics have been observed in ultrafast fiber lasers, such as evolution of femtosecond soliton molecules, the internal motion of dissipative optical soliton molecules, and the dynamics of soliton explosions.

Among these researches, CNT-SA is a key component that suppresses the environmental perturbation and optimizes the laser system to reveal the true highly stochastic and non-repetitive unstable phenomena of the initial self-starting lasing process. This review is intended to provide an up-to-date introduction to the development of CNT-SA ultrafast fiber lasers, with emphasis on recent progress in real-time buildup dynamics of solitons in CNT-based mode-locking fiber lasers. First of all, we briefly look into the characteristics of CNT-SA. Secondly, we discuss the application of CNT-SA for ultrafast fiber lasers and the current development of CNT-SA fiber lasers. Next, with the benefit of CNT-SA, we go to the details of experimental real-time observation of buildup dynamics of solitons in ultrafast lasers. Finally, we provide in-sights into further research directions and the current challenges.

2 Carbon nanotube-based saturable absorber

CNT is a kind of one-dimensional nanomaterial with remarkable electrical, thermal, mechanical, and optical properties. It was firstly reported by Iijima et al. in 1991, which was a multi-walled CNT (MWCNT) [23]. The single-walled CNT (SWCNT) was discovered simultaneously and independently by Iijima et al. from Japan and Bethune et al. from America in 1993 [24, 25]. The morphology of SWCNT is considered to be a single graphene sheet but rolled up into seamless hollow cylinders. This unique structure, which can enable SWCNT with remarkable physical (electrical and optical), chemical, and mechanical properties, has attracted tremendous attentions from physicists, chemists, and material scientists, and has become a research hotspot in science and engineering that continues to this day. The roll direction of the graphene sheet determines the band structure of SWCNT. Its electronic conduction shows several properties from semiconductor to metal, which depends on the diameter and chirality of the graphitic arrangement of CNTs [26] as shown in Figure 1(A). For semiconducting SWNT, the band gap width is inversely proportional to the pipe diameter, which is known as kataura plot as shown in Figure 1(D) [27]. The common synthesis methods of CNT include arc discharge, CVD, laser ablation, and high pressure carbon dioxide reduction [12, 28]. Generally, the SWCNT obtained is a mixture with a variety of pipe diameter, including both semiconducting SWCNT and metallic SWCNT, of which the metallic one

accounts for about 1/3 [29, 30]. At the same time, the semiconducting SWCNT has a certain diameter distribution, so that it can correspond to a number of different wavelengths.

Saturable absorption is the phenomenon that the absorption of light by matter decreases with the increase of incident light intensity. Most materials maintain saturable absorption characteristics, but they usually need very high light intensity, even close to or higher than the damage threshold. When the light incident on the semiconductor material, the carrier of the valence band will be excited to transition to the conduction band, which is the absorption of light. When the incident light intensity increases, the carrier of valence band is depleted (p-type doping) or the conduction band is filled (n-type doping) according to the different characteristics of materials. Due to the Pauli incompatibility principle, two electrons cannot have the same electronic state, which hinders the continuous absorption of light by the material. At this time, the absorption of light by the semiconducting material reaches the saturation state.

The semiconducting SWCNT has similar bandgap structure compared with the semiconductor and has excellent saturable absorption properties. In addition, CNT has advantages of fast recovery, low saturation intensity, polarization insensitivity, deep modulation depth, broad operation bandwidth, outstanding environmental stability, and affordable fabrication. These characters make CNT ideal SA for ultrafast lasers. However, there are several problems that hinder the practical application of CNT as SA. In the process of SWCNT synthesis, the content of CNTs is relatively low, which usually needs further enrichment and purification. The wide distribution of pipe diameter will lead to additional unsaturated absorption loss, and the repeatability of preparation is not good. Due to the high surface energy of CNT, the nanotubes are easy to agglomerate into clusters. The particle size of CNTs is equal to the order of light wavelength, which will produce a large loss. The axial thermal conductivity of CNT is very good, but the thermal conductivity between tubes is very poor, which will lead to oxidation and combustion in the air at about 400 °C, seriously affecting the damage threshold characteristics of CNTs mode-locker.

In order to effectively utilize the nonlinear absorption characteristics of CNT in fiber lasers, researchers have designed a variety of SWCNT-based mode-locker, which can be divided into two types: transmission-type and evanescent field type. Transmission-type refers to the integrated way of passing light vertically through SWNT, while the most commonly use one is the fiber ferrule integrated type [28, 36, 37] as shown in Figure 2(C). In this way, it is usually necessary to mix the CNT with composite film, which can prevent the agglomeration of SWNT in the preparation process, and isolate SWNT from air and prevent oxidation. The commonly used polymers are polyvinyl alcohol (PVA), polystyrene, polymethylmethacrylate, epoxy resin, and polycarbonate [10, 28]. The optical deposition method can also be used to make SWNT evenly coated on the end face of the optical fiber, which is easy to be damaged since it is exposed to the air [38]. In addition, Martinez et al. designed the microfluidic channel type on the optical fiber and filled the CNT dispersion into it to obtain an SWNT mode-locker with compact structure [31]. The fabrication of evanescent field type mode-locker is usually based on the evanescent field interaction on the surface of D-type fiber or micro/nano fiber [32, 33]. Compared with the transmission type, the damage threshold power of evanescent field type mode-locker is

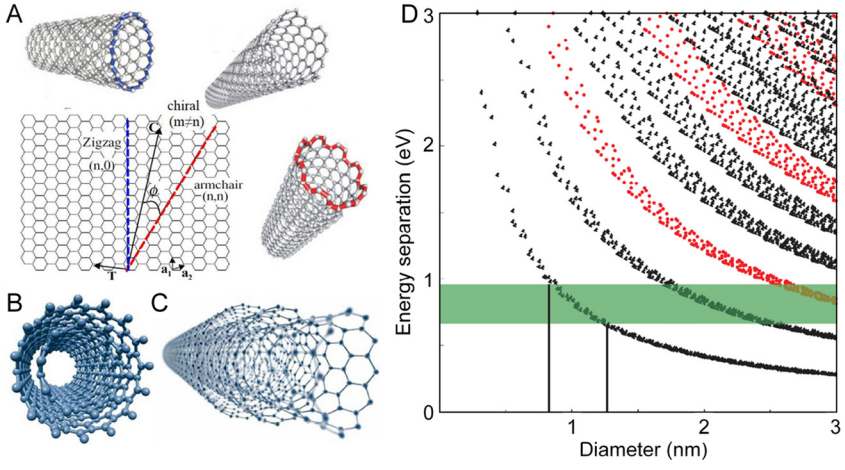

Figure 1: Fundamentals of CNTs: (A) Structures SWCNT in function of chirality (zigzag, armchair, and chiral); (B) Structure of DWCNT; (C) Structure of MWCNT made up of several concentric shells, Tîlmaciu et al. [22]. © Tîlmaciu and Morris 2015; (D) Kataura plot, each point represents a different diameter and chirality of the graphitic arrangement of SWCNTs, the black and red dots represent semiconducting and metallic nanotubes, respectively. The green region shows semiconducting nanotubes with diameters between 0.8 and 1.3 nm can be used for saturable absorption in telecommunications window (1300~1600 nm). Adopted from: https://www.photon.t.u-tokyo.ac.jp/~maruyama/kataura/kataura.html.

significantly increased, and the interaction distance between optical field and SWNT is extended, which is conducive to making full use of the nonlinear effect of mode-locked materials. Moreover, other evanescent field type mode-lockers have been constructed by using hollow fiber [34] and holey fibers [35]. However, the evanescent field type CNT-SA usually has higher saturation intensity.

There are numerous works that have discussed the saturable absorption property in detail [7, 10, 12, 28, 39–41]. Here, we highlight the low saturation intensity of CNT-SA, which is advantageous to achieve mode-locking while prevent Q-switching instabilities [5] and also benefit to the CNT-SA based fiber lasers to run with high stability, reliability, and excellent self-starting performance. The saturation intensity of SWCNT is typically in the level of ~10 MW/cm^2, which is comparable with SESAMs [37]. Compared with its counterparts, e. g., graphene, this value is more than one orders lowers than that of graphene SA. It is also advantageous compared with other emerging 2D materials [42, 43]. The CNT-SA based mode-locked fiber lasers have high stability and reliability, it can run continuously for over 200 h without significant degradation of average power and spectral width [44]. Our homemade CNT-SA mode-locked fiber laser shows ultrahigh reliability, it can help to suppress the Q-switched lasing induced by the environmental perturbation, restore the entire buildup process of soliton buildup, and enable the measurement of the entire buildup dynamics of soliton of the laser, which is described in detail in Section 4. CNT-SA mode-locked fiber laser is resistant to the environmental perturbation, as shown in supplement 1–3, it is immune to be shaking of the laser setup, it can also restore to the stable state after press the intra-cavity fiber.

3 CNT-based ultrafast fiber laser

Due to the excellent properties for saturation absorption, CNT-SA has been widely used in Q-switched and mode-locked lasers, including the solid-state lasers [45–49], semiconductor lasers [50], waveguide lasers [51], and fiber lasers. The excellent properties of CNT-SAs enable ultra-stable, ultrashort, and compact fiber laser system working from the visible to the mid-infrared spectral region [52–55], with functionalized operations like gigahertz repetition rate [56–58], multi-wavelength output [36, 59, 60], pulse duration, and spectral bandwidth tunability [37, 61–65]. Various operation regimes, including Q-switching [52, 53, 66–71], Q-switched mode-locking [72], and mode-locking [9, 37, 50, 73–76], were reported. Pulse evolution and interaction dynamics, including various soliton types [9, 37, 55, 77–79], soliton molecule [74, 80, 81], harmonic mode-locking [58, 75, 82], vector solitons [83, 84], dark soliton [85], and soliton rains [86, 87], were observed based on SWCNT-SAs and MWCNT-SAs. Due to the technical advantages of high beam quality, high efficiency, high integration, high reliability, etc., of fiber lasers, in this section, we mainly focus on the CNT-SA-based ultrafast fiber lasers. A summary of the progress of CNT-SA mode-locked fiber lasers is shown in Table 1.

3.1 CNT-based Q-switched fiber laser

Fiber lasers using Q-switching technique can produce pulses with high energy, pulse duration ranging from micro- to nano-seconds and repetition rates typically around kilohertz. The mechanism of Q-switching is quality factor

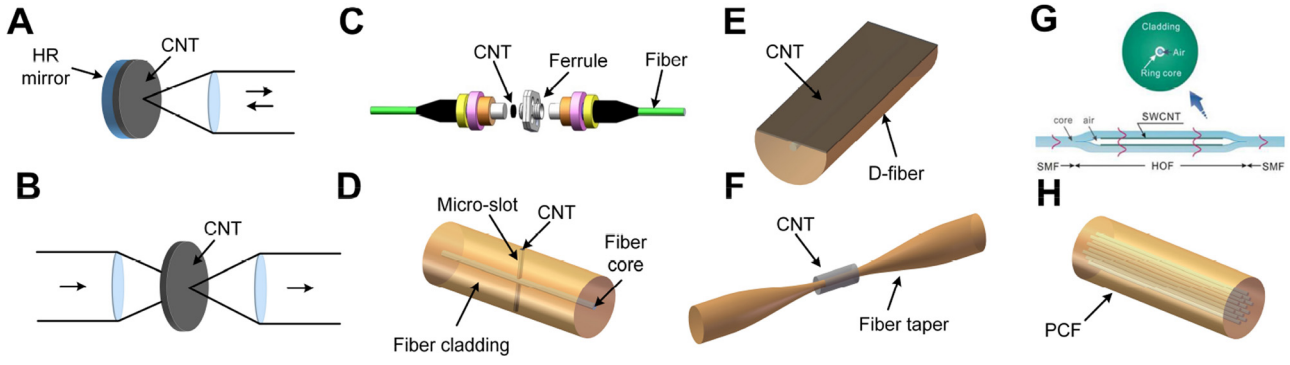

Figure 2: Schematic diagram of the CNT mode-locking device: (A–D) Transmission type; (E)–(F) evanescent field type; (A) Reflection type; (B) transmission type; (C) fiber ferrule integrated type; (D) microfluidic channel type, Martinez et al. [31]. © Optical Society of America 2008. (E) Based on D-type fiber, Song et al. [32]. © Optical Society of America 2006; (F) based on micro/nano fiber, Song et al. [33]. © American Institute of Physics 2007; (G) Based on hollow fiber, Choi et al. [34]. © Optical Society of America 2009; (H) Based on holey fiber. Obraztsova et al. [35]. © John Wiley & Sons, Inc 2010.

Table 1: Progress of CNT-SA mode-locked fiber laser.

SA	Gain fiber	Soliton	wavelength (nm)	Bandwidth (nm)	width (fs)	Energy (pJ)	Average power (mW)	Repetition rate (MHz)	Ref.
SWNT-P3HT-PC	EDF	CS	1560	13	193	\	0.9	\	[9]
CNT-PVA	EDF	CS	1560	\	178	68	\	22.8	[118]
SWNT-PC	EDF	CS	~1500	24.6	115	\	3.4	39.1	[119]
Deposit on endface	YDF	CS	1070	7.2	137	5	0.1	20.1	[38]
Deposit on endface	EDF	CS	1570.4	5.32	332 ns	340	0.31	909.1 kHz	[120]
CNT-PVA	YDF	CS	1042	1.3	1.23 ns	\	\	641 kHz	[121]
Microchamber CNT	EDF	CS	1564	0.24	3.37 ps	11 nJ	29	2.3	[122]
Evanescent field	EDF	CS	1563	2.6	1.02 ps	6.5 nJ	250	38.9	[44]
CNT-PVA	BDF	CS	1177	0.35	4.7 ps	3 pJ	\	5.13	[124]
Purified CNT	PDF	CS	1294	0.15	11.7 ps	\	1.67	3.18	[125]
CNT-CMC	TDF	CS	1733–2033	4.3–0.6	0.9–6.4 ps	\	1	14.83	[65]
m-SWCNT	HDF	CS/StP/SsP/DS	~2080	6.65 for CS 37 for StP	683 for CS 212 for StP	376 pJ for CS 3.79 nJ for StP	20.5 for CS 84 for StP	54.52	[127]
Deposit on mirror	HPDF	\	~2865	1.4	\	\	71.8	12.7	[53]
CNT-CMC	EDF	StP	~1550	63	74	36	1.2	33	[135]
Evanescent field	EDF	StP	1554	54	66	178	26	146	[136]
C: BNNT	EDF	SsP	1560	44	127	200	7.14	38.117	[150]
Evanescent field	YDF	DS	1085	6.2–16.3	25.6–62.6 ps	1.6–29 nJ	9–162	5.59	[164]
Evanescent field	EDF	DS	1563	12.1	12.7ps	34 nJ	335	9.8	[151]
Deposited on mirrors	EYDF	CS	1563	4.3	680	\	~6.3	19.45 GHz	[56]
CNT-PVA	EDF	StP	1595.63	9.1	863	2.41 nJ	5.83	2.415 GHz	[58]
SWNT–PC	EDF	CS	1518–1558	1.2	2.39 ps	24	0.36	15	[37]
CNT-PVA	EDF	CS	1528–1552	0.3	~7–150 ps	\		\	[61]
CNT-CMC	EDF	CS	1525–1559	1.2	545 fs–6.1 ps	\	15	62	[64]

modulation to store and release the energy in the laser cavity. The stability criterion of passively CW Q-switching is determined by the cavity length, gain material, and the SA [5, 88–90]. For the SA, the large modulation depth, saturation intensity, mode area [5], and recovery time [88] are preferred for Q-switched operation. The CNT-SAs, can be designed with large modulation depth, have both a fast and a slow response time, can be used for passively Q-switched fiber lasers. Since the first report of CNT-SA in 2003 [8], many works have been done to extend the wavelength, pulse energy, pulse width, repetition rate of Q-switched fiber lasers, etc., and endowed them with tunability, multi-wavelength output, by improving the cavity, and the CNT-SA fabrication and implementation method.

The first demonstration of CNT-SA based Q-switched fiber laser was reported by Set et al. in 2003 [91]. The results reported a dual-regime laser operation, with mode-locking operation at low pump power, while Q-switching operation by improving the pump power from mode-locking regime. By raising the pump power, the repetition rate of pulse train varies from 34.55 to 37.45 kHz, and the pulse width varies from 5.32 to 4.04 μs. A similar dual-regime operation was also reported by Li et al. in 2014 [67], the transitioning from mode-locking to Q-switching at high pump power was explained by the optical limiting effect of the CNT-SA due to the variation of nonlinear transmission. Active control of the operation regimes can also be achieved by employing a fast Si-based variable optical attenuator [72] and by adjusting polarization controller in front of the specially fabricated polarization dependent CNT-SA, where the CNT-SA is implemented by synthesizing well-aligned CNT arrays using zeolite AlPO4-5 as a mask [68, 92].

Up to now, CNT-SA-based passively Q-switched fiber lasers can produce pulse energies over 100 nJ [53, 71, 93–95] and even up to 1.7 μJ in Tm-doped fiber laser using a "Yin-Yang" all-fiber cavity [69], pulse durations from μs to ~300 ns [96, 97], and repetition rate up to 178 kHz [53]. Wavelength tunability can be endowed by using the tunable band pass filters [98–100] or gratings [71] in the related spectral regions.

The operating wavelength of the CNT-SA-based Q-switched fiber lasers is mainly determined by the gain medium and the absorption band of CNT-SA. The nonlinear optical absorption region of CNT can be customized through controlling the diameter and chirality of the nanotubes. Generally, CNT-SAs are mainly fabricated to work across 1.0~2.0 μm region. Hence, CNT-SA based passively Q-switched fiber lasers are mainly demonstrated in this region, including ~1060 nm using ytterbium (Yb)-doped fiber [67, 94, 100–102], ~1300 nm using the praseodymium (Pr)-doped fluoride fiber [98], ~1550 nm using the erbium (Er)-doped fiber [92–96, 99, 102–110], ~1900 nm using the thulium (Tm)-doped fiber [66, 69, 93, 111–113], 2097 nm using the holmium (Ho)-doped fiber [97]. In 2016, Xu et al. reported that nonlinear absorption wavelength of SWCNT could extend into the visible region [114]. Following this work, Li et al. successfully demonstrated red light Q-switched all-fiber Pr:ZBLAN fiber laser using an SWCNT/PVA as the SA, based on the linear fiber cavity and bidirectional ring cavity configurations, and pumping with 445 nm laser diode, they achieved the output at wavelength of 716 [70], 635.4 nm (Figure 3 (A)) [52], respectively. Recently, spectral region of CNT-SA based passively Q-switched fiber lasers has been extended to mid-infrared. By using the SWCNT-SA with nanotube diameters around 1.5 nm, Lyu and coworkers successfully demonstrated CNT-SA based Q-switching in a Ho/Pr-codoped ZBLAN fiber operating in the wavelength of ~2.8 μm with wideband tunability [53, 71].

3.2 CNT-based passively mode-locked fiber laser

3.2.1 CNT-SA based soliton fiber laser

In mode-locked fiber lasers, ultrashort pulses have high peak power and thus generate high nonlinear phase shift. If the accumulated nonlinear phase shift cannot be controlled or compensated by dispersion, it will cause wave breaking, that is to say, the pulse splits or collapses into noise like pulse [115]. In order to get high-energy pulses, it is necessary to control the nonlinear effect in the laser reasonably. One way to control the nonlinear phase shift is to increase the area of the fiber mode field and reduce the energy density. The other is to control the nonlinearity and dispersion in the laser cavity. The dispersion in the cavity varies with the position, which is called dispersion map. According to the dispersion distribution characteristics of the fiber laser, the CNT-based mode-locked fiber laser can produce conventional soliton (CS), stretched pulse (StP), self-similar pulse (SsP), and dissipative soliton (DS). The net cavity dispersions are β_{net}<0 ps^2, β_{net}≈0 ps^2, β_{net}≈0.01 ps^2, β_{net}>>0.01 ps^2, respectively. The temporal profiles of these four kinds of solitons are sech^2, Gaussian, parabolic, super-gaussian, while pulse energies usually are in the level of ~0.1 nJ, ~1 nJ, ~10 nJ, ~50 nJ, respectively.

3.2.1.1 Conventional soliton

In most conditions, the CNT-SA based mode-locked fiber lasers are operating in anomalous dispersion regime with

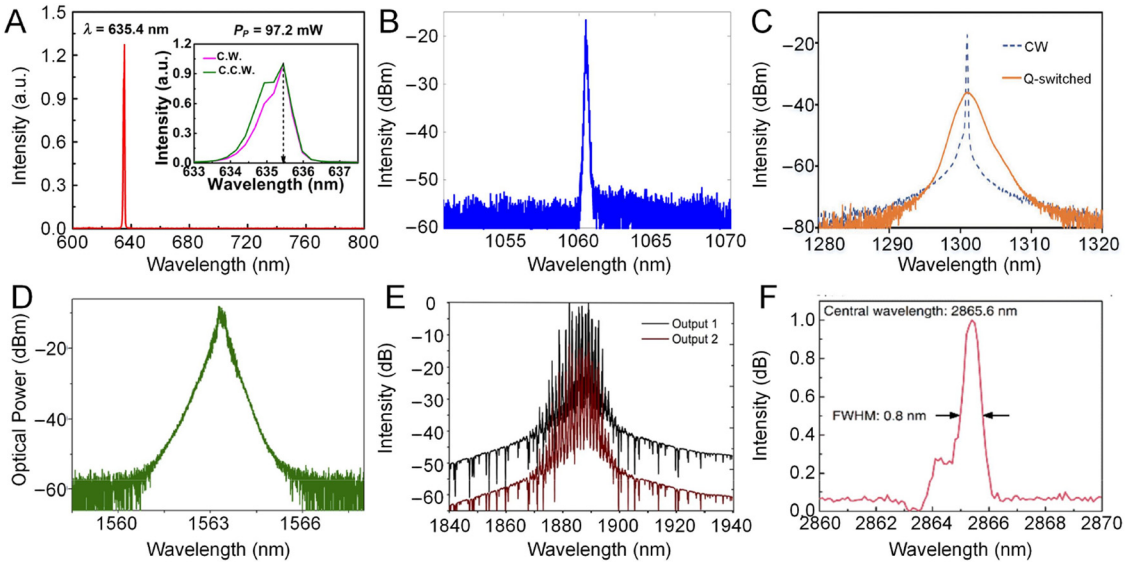

Figure 3: CNT-SA based Q-switched fiber laser covering the spectral region from visible to mid-infrared. (A) 635 nm based on Pr:ZBLAN fiber, Li et al. [52]. © IEEE 2018; (B) ~1060 nm based on Yb-doped fiber, Li et al. [67]. © Optical Society of America 2014; (C) 1300 nm based on Pr-doped fluoride fiber, Ahmad et al. [98]. © Chinese Physical Society and IOP Publishing Ltd 2019; (D) ~1560 nm based on Er-doped fiber, Xu et al. [68]. © Elsevier Ltd 2015; (E) ~1900 nm based on Tm-doped fiber, Chernysheva et al. [69]. © Springer Nature 2016; (F) ~2800 nm based on Ho /Pr co-doped ZBLAN fiber, Wei et al. [53]. © IEEE 2019.

the balance between dispersion and Kerr nonlinearity, in addition to the gain and loss in the cavity, and thereby can form soliton-like pulses, which are also named as CSs. The CSs are close to transform limit, with clear Kelly sidebands in the spectral domain and $sech^2$ profile in the temporal domain. Most of the research on pulses operating in CS regime focuses on testing the characteristics of CNT-SAs in various parameters and implementations, revealing the pulse evolution dynamics, improving the output performance of lasers (repetition rate, pulse duration, pulse energy, wavelength), and endowing them with various functions.

The first demonstration of CS generated by CNT-SA based mode-locked fiber lasers was reported by Set et al. [8], extended from the application of noise suppressing [116], and studied in detail later in [117]. From then on, conventional solitons based on CNT-SA fiber laser are widely explored. The typical pulse durations of CS are between 200 fs and 1 ps, spectral width <5 nm, pulse energy in the level of 100 pJ, average output power in the level of 1 mW at repetition rate of several to tens of megahertz (MHz). Up to now, the pulse duration of CSs in CNT-SA based mode-locked fiber lasers have been shortened to sub-200 fs at ~1550 nm in Er-doped fiber [9, 118, 119]. At the operation wavelength of ~1 μm, it has been shortened to 137 fs [38]. While most attentions were focused on the ultrafast CNT-SA mode-locked fiber lasers, several works focused on producing solitons with pulse duration on the nanosecond scale [120, 121] using the long cavity configuration, as it has advantages of high pulse energy and average power for applications like mid-infrared pulse generation. The single pulse energy has been improved to 11 nJ with pulse duration of ~3.37 ps [122], the average power and peak power have been improved to 250 mW and 5.6 kW at repetition rate of 38.9 MHz [44].

The operation wavelengths of fiber lasers have covered ~1000 nm using Yb-doped fiber [128],1177 nm using bismuth (Bi)-doped fiber [124] ~1300 nm using Pr-doped fiber [125], ~1550 nm using Er-doped fiber [9, 117, 129, 130], ~1900 nm using Tm-doped fiber [65, 131, 132], ~2100 nm using Ho-doped fiber laser [133]. Recently, Ho-doped mode-locked fiber laser based on metallic CNT-SA has been demonstrated [127]. In this work, the authors used complex band structure of individual bundled nanotube in thin films to open the bandgap and enable optical absorption in near-infrared spectral range in metallic CNTs. Finally, transform limited CSs with spectral bandwidth of 6.6 nm, pulse duration of 683 fs at wavelength of ~2080 nm were obtained.

In these reports, nonlinear absorption performances of the CNT-SAs are tailored by controlling the structure and the diameters of nanotubes. Interestingly, by using a distribution of different nanotube diameters of SWCNT in a single SA, wideband ultrafast optical pulse generation that potentially covers 1–2 μm spectral region can be achieved. As shown in Figure 4(A)–(D), Kivistö et al. have fabricated

a novel polymer-free SWCNT-SA with diameter of tubes ranging from 1.2 to 1.8 nm [54]. The same SWCNT-SA was assembled in the linear fiber cavity to achieve mode-locking using Yb, Er, and Tm: Ho-doped fiber laser, respectively. In the three mode-locked lasers using the same SWCNT-SA, sub-picosecond pulses operating at 1.05, 1.56, and 1.99 μm were demonstrated, respectively. By properly designing the outer and inner wall electronic types and controlling the nanotube diameters of DWCNT-SA, Hasan and the coworkers have also reported another wide-band mode-locked fiber laser operating at 1066, 1559, and 1883 nm [55], as shown in Figure 4(E)–(H).

In recent years, mid-infrared laser, especially operating at 3~5 μm band, has been widely concerned and studied due to its characteristics of molecular fingerprint area, atmospheric window area, human eye safety area. It has important application value in biomedical, laser detection, spectral analysis, laser communication, national defense security, and other fields. However, CNT-SA mode-locked fiber lasers are limited to the near-infrared region. Recently, Wei et al. demonstrated that the CNT-SAs can be promising for mid-infrared pulsed lasers [53, 134]. The fabricated CNT-SA showed strong nonlinear transmission at 2850 nm, the measured modulation depth is 16.5%, saturation intensity is 1.66 MW/cm^2, and the non-saturable loss 71.8%. Using Ho/Pr-codoped ZBLAN fiber, the laser shown both Q-switching and mode-locking operations, the mode-locked pulses had spectral bandwidth of 1.4 nm at 2865.2 nm.

3.2.1.2 Stretched pulse

The CS has become one of the most important topics in the research of mode-locked fiber laser in the past few decades. However, it has serious inherent disadvantages: pulse energy cannot be scaled up, while the maximum single pulse energy is usually less than 0.1 nJ. When the pulse energy is higher, the pulse will split and thereby form multi-pulse or pulse collapse. Moreover, the pulse duration of CS is usually between 0.2 and 1 ps, further reducing the pulse duration is difficult. One effective method to simultaneously increase the pulse energy and reduce pulse duration is using dispersion management in the cavity. In the dispersion managed fiber cavity, the net dispersion is very close to zero. With alternating anomalous and normal dispersion using different type of fibers, the mode-locked pulse can be periodically broadened and compressed. This method can effectively reduce the peak power of the pulse in the cavity, thus inhibiting pulse splitting caused by nonlinear effect, and obtaining much high energy pulse [137, 138]. In addition, the pulse width and spectrum at different positions in the resonant cavity would change dramatically. The maximum and minimum pulse width could differ by tens of times. After compression, pulse duration can be less than 100 fs. This kind of dispersion managed pulses is also known as the StPs, with no Kelly sidebands in the spectral domain and Gaussian-like profile in the temporal domain.

There are a few works that report the CNT-SA StP generation [77, 127, 135, 136, 139, 140–149], showing that

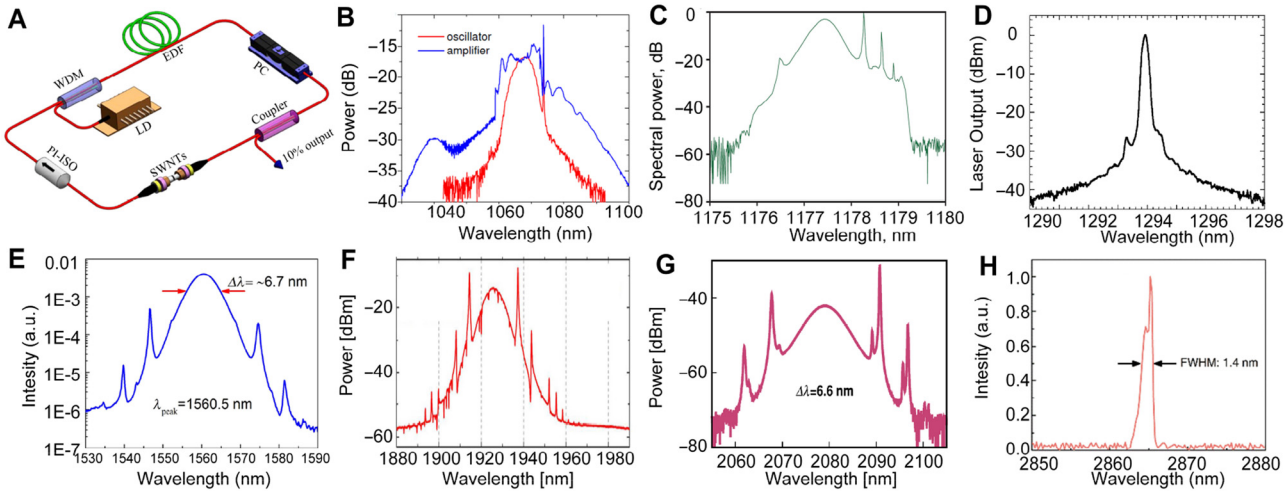

Figure 4: CNT-SA mode-locked fiber laser covering the spectral region from near-infrared to mid-infrared: (A) typical schematic diagram of CNT-SA mode-locked fiber laser. Yao et al. [123]. © IOP Publishing 2014; (B) ~1000 nm using Yb-doped fiber laser. Nicholson et al. [38]. © Optical Society of America 2007; (C) 1177 nm using Bi-doped fiber laser. Kelleher et al. [124]. © IOP Publishing 2010; (D) ~1300 nm using Pr-doped fiber laser. Song et al. [125] © IEEE 2005; (E) ~1550 nm using Er-doped fiber. Li et al. [64]. © Springer Nature Limited 2018; (F) ~1900 nm using Tm-doped fiber laser. Sobon et al. [126]. © Springer Nature Limited 2017; (G) ~2100 nm using Ho-doped fiber laser. PAWLISZEWSKA et al. [127]. © Optical Society of America 2019; (H) mid-infrared using Ho/Pr-codoped ZBLAN fiber laser. Wei et al. [53]. © IEEE 2019.

the common pulse durations are <200 fs, spectral width >20 nm. The first demonstration of CNT-SA StP generation was presented in 2009 [144], and the detailed demonstration was shown in [146]. The laser generated StP at 1.56 μm with pulse duration of 113 fs and spectral width of 33.5 nm. To achieve narrower pulse duration or wider spectral width, it is useful to adopt highly doped broadband gain medium and a short cavity. In this way, Popa et al. demonstrated the generation of StP with spectral width of 63 nm and pulse duration of 74 fs, however, pulse energy of only 36 pJ [135] as shown in Figure 5(A)–(B). To obtain higher pulse energy and to increase the CNT-SA optical damage threshold, Yu et al. adopted the SWCNT-SA using the evanescent field interaction in a microfiber in a shorter length Er-doped laser cavity (1.2 m) [136] as shown in Figure 5 (C)–(D). The produced StPs energy was raised to 0.18 nJ with average output power of 26 mW at 1555 nm. The pulse duration is 66 fs with spectral width of 54 nm, which is to data, the shortest pulse in CNT-SA mode-locked fiber lasers. In addition, StPs has been obtained in Yb-doped fiber laser at 1025.5 nm [142] and Tm-doped fiber laser at ~2 μm [77, 143]. In the metallic CNT-SA for Ho-doped fiber lasers, the StPs were produced with 31.4 nm spectral width, 212 fs pulse duration, and 3.79 nJ pulse energy at ~2080 nm [127].

3.2.1.3 Self-similar pulse and dissipative soliton

In recent year, similariton (self-similar) mode locking [152] and dissipative mode locking [17] have been developed to obtain higher pulse energy directly from the mode-locked fiber laser. In general, self-similar pulse (SsP) has parabolic-like profile and can be generated in slightly normal dispersion regime. During the intracavity evolution of SsP, the spectral width will be greatly broadened and spectral filtering or spectral compression mechanisms must be introduced to realize the mode-locked output of SsP. DSs have super-gaussian profile and can be generated in large normal dispersion regime, under combined effects of gain medium spectral filtering effect, Kerr nonlinear effect, dispersion, SA, gain, and loss. Compared with CS and StP, SsP and DS can tolerate much stronger nonlinearity, thus can effectively avoid the pulse splitting, break through the energy limitation of the traditional fiber lasers, and achieve higher energy pulse output.

There are only a very few researches on CNT-SA based SsP generation [78, 150, 153], mainly due to the difficulties of dispersion control and the requirement of extra spectral filter. Here, we highlight the SsP generation in the Er-doped fiber laser mode-locked by NPE mechanism in conjunction with CNT-SA, as shown in Figure 6(A)–(C) [150]. In the cavity, the NPE was completed by locating two polarization controllers at both ends of the birefringent "PANDA"-type silica-glass fiber (PZ-fiber). The net cavity dispersion is controlled to be ~0.01 ps^2 at 1560 nm, which is important for SsP generation. The laser generated stable SsP at 1560 nm with 44 nm spectral width and 127 fs pulse duration, the pulse energy was 0.2 nJ, maximum peak power of 1.5 kW and average output power of 7.14 mW. Moreover, it showed very low repetition rate deviation.

DS in CNT-SA based mode-locked fiber laser was first demonstrated by Kieu et al. in 2008 [79], the all-fiber normal-dispersion Yb-doped fiber laser using CNT-SA that implemented by fiber taper embedded in a CNT/polymer composite can generate DS with pulse duration of 1.5 ps, pulse energy of 3 nJ and can be dechirped to 250 fs outside the cavity. Wavelength switchable and tunable DS Yb-doped fiber laser has also been proposed [154]. To produce DS in Er-doped fiber laser, dispersion compensating devices, such as chirped fiber brag grating (CFBG), dispersion compensating fiber (DCF), are necessary to manage the cavity dispersion [151, 155–159]. DS in CNT-SA based mode-locked fiber lasers operating at 1.32 μm using Bi-doped fiber

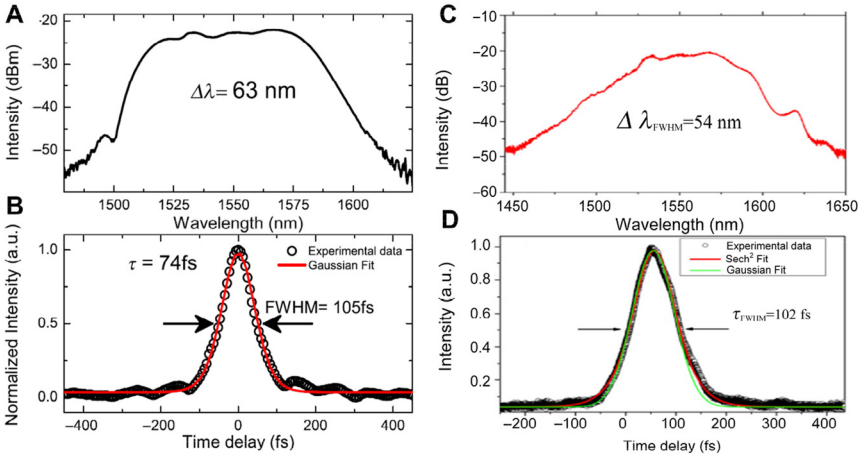

Figure 5: Laser output of the StPs at ~1.55 μm from the CNT-SA mode-locked fiber laser: (A)–(B) Laser output with spectral width of 63 nm and pulse duration of 74 fs, Popa et al. [135]. © American Institute of Physics 2012; (C)–(D) Laser output with spectral width of 54 nm and pulse duration of 66 fs, Yu et al. [136]. © IOP Publishing 2020.

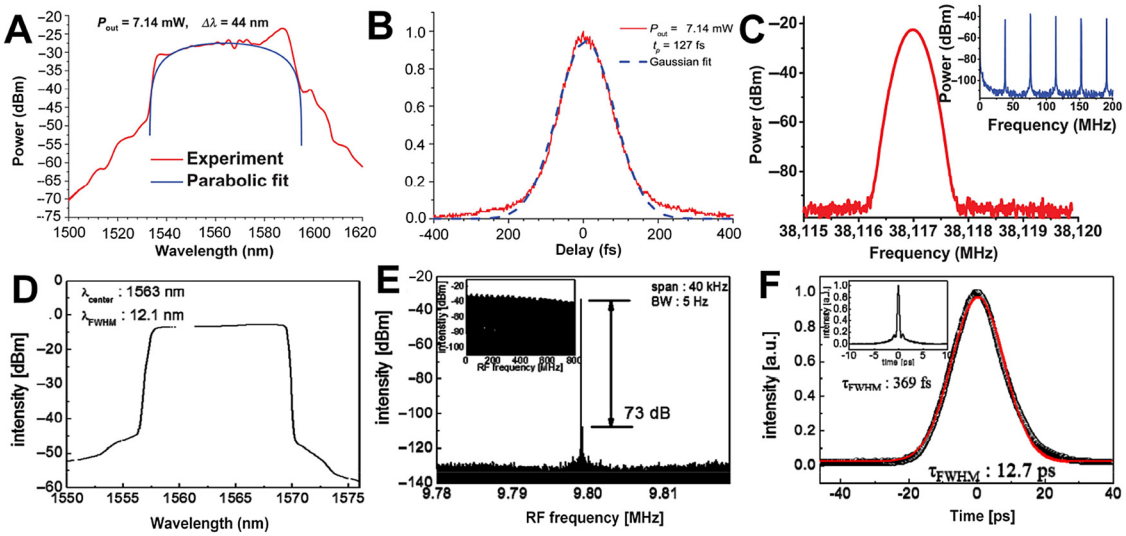

Figure 6: Laser output of the SsPs and DSs at ~1.55 μm from the CNT-SA based mode-locked fiber laser. (A)–(C) Optical spectrum, autocorrelation and radio frequency spectrum of SsPs, Lazarev et al. [150]. © IEEE 2016; (D)–(F) Optical spectrum, radio frequency spectrum and autocorrelation of DSs, Jeong et al. [151]. © Optical Society of America 2014.

[160], 1.9 μm using Tm-doped fiber [77, 161], and 2.08 μm using Ho-doped fiber [127] have also been reported. To further extend the working wavelength, CNT-SA based Raman lasers have been proposed, which can cover the wavelength of 1.12 and 1.666 μm [162, 163]. For high energy DS generation, CNT-SA based on evanescent field interaction is preferred, since it can sustain higher optical damage threshold. By depositing the CNT-SA on D-shaped fibers, energy of DS in Yb-doped fiber laser has been raised to 29 nJ with stable operation at 1085 nm using the large modulation depth (51%) CNT-SA [164], while in Er-doped fiber lasers, pulse energy as high as 34 nJ at 1563 nm can be obtained [151] as shown in Figure 6. However, it is still challenging for achieving higher energy self-similar pulse and dissipative solitons in CNT-SA mode-locked fibers due to the relatively low optical damage threshold of the present CNT-SA.

3.2.2 High repetition rate CNT-SA mode-locked fiber lasers

Ultrafast lasers with high repetition rate have many potential applications in fields of optical telecommunications, frequency metrology, high-speed optical sampling, and data storage [165–167]. However, as mentioned above, fiber lasers usually have a fundamental repetition rate of several to tens of MHz. There are two effective methods to increase the pulse repetition rates: one is shortening the laser cavity length; the other less technically challenging and more convenient way is the harmonic mode-locking (HML) [57, 58, 75, 82, 168, 169]. By shorten the fiber laser cavity length, Martinez et al. have increased pulse repetition rate to GHz and even up to 10 GHz [170] and 19.45 GHz [56], the laser setup and optical spectrum are shown in Figure 7(A)–(B). By shortening the Fabry–Pérot laser cavity length to 5 mm, the fundamental repetition rate was increased to 19.45 GHz.

Compared with shortening the cavity length, passive HML has the intrinsic advantage of repetition-rate self-stabilization. The formation of HML is mainly due to the soliton interactions in the cavity. Recently, we have revealed the buildup dynamics of HML in CNT-SA mode-locked fiber laser based on the TS-DFT technique. By means of the optoacoustic effect that induces a trapping potential, the acoustic resonance can stabilize the mode-locking of laser at different harmonics (from the first to sixth order at the appropriate pumping strength) with perfect long-term stability [75]. Up to now, the repetition rate using HML has been increases to 2.415 GHz at 1594.97 nm with 40 dB side mode suppression ratio (SMSR), which corresponds to 213rd harmonic of the fundamental cavity repetition rate [58] as shown in Figure 7(C)–(H).

3.2.3 Tunable and multiwavelength CNT-SA mode-locked fiber lasers

For various applications like fiber telecommunication, optical sensing, metrology, and microscopy, ultrafast lasers with controllable flexible pulses, such as wavelength

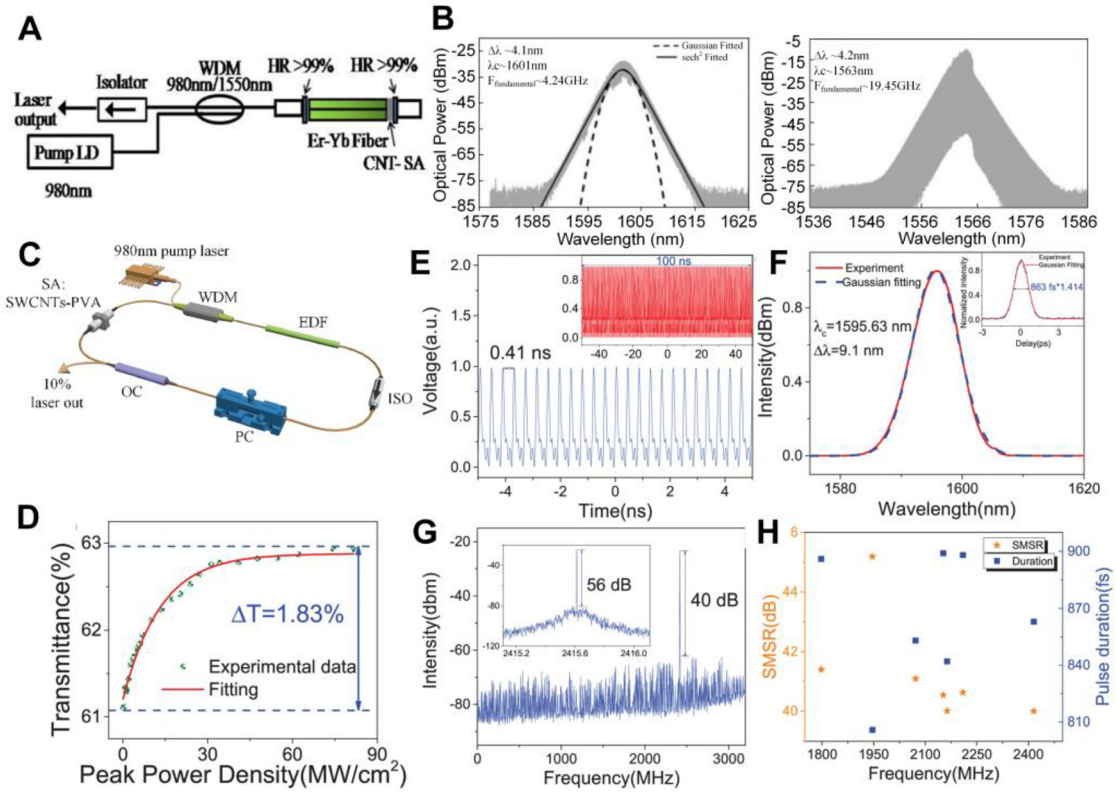

Figure 7: High repetition rate CNT-SA mode-locked fiber lasers: (A) CNT-SA based high repetition rate laser using short Fabry–Pérot cavity; (B) Optical spectrum of the laser using short Fabry–Pérot cavity at repetition rates of ~4.24 and ~19.45 GHz with cavity length of 25, 10, and 5 mm, respectively, Martinez et al. [56]. © Optical Society of America 2011. (C) SWCNT-SA based Harmonic mode-locking laser; (D) nonlinear transmission of the CNT; (E) oscilloscope results; (F) Optical spectrum; (G) Radio frequency spectrum showing the repetition rate of 2.415 GHz; (H) The variations of SMSR and pulse duration when pulses frequency ranges from 1.8 to 2.415 GHz, Huang et al. [58]. © IEEE 2020.

and pulse width tunable, multiwavelength output, wavelength switching, and bidirectional output are desired. A variety of technologies have been proposed to achieve wavelength or/and pulse width tunability in CNT-SA mode-locked fiber lasers, including tunable band pass filter (TBPF) [37, 64, 171, 172], fiber Bragg grating [61], CFBG [62], 45°tilted fiber grating [173], diffraction grating mirror [63, 65], and tunable Lyot filter [154, 174]. Wavelength tunable range is related to the SA operating bandwidth, gain bandwidth of gain medium, and also the performance of the tuning devices. Due to the advantage of broad operating wavelength of CNT, wavelength tunable CNT-SA mode-locked fiber lasers have covered the 1~2 μm spectral region with up to 40 nm tuning range in Er-doped fiber lasers while 300 nm in Tm-doped fiber laser, tuning range of pulse duration has covered the 360 fs to 150 ps [61, 64, 65, 174] with typical results shown in Figure 8.

Multiwavelength operation in CNT-SA mode-locked fiber lasers is mainly focused on Er-doped fiber laser, using the 1530 and 1560 nm dual-wavelength band by tuning the cavity loss [59, 60, 175, 176]. We have proposed versatile multi-wavelength CNT-SA mode-locked fiber laser by using the CFBGs [36]. The laser adopted three CFBGs with different central wavelength. The output central wavelengths are 1539.5, 1549.5, and 1559.5 nm, respectively, which can be accurately selected by CFBGs. Output wavelengths are tunable by stretching CFBGs. Pulse durations of three wavelengths are 6.3, 6.7, and 5.9 ps, respectively.

3.2.4 Dynamics of solitons in CNT-SA mode-locked fiber lasers

In addition, mode-locked fiber lasers can work as excellent platform to investigate a variety of soliton dynamics. These soliton dynamics could reveal the underlying mechanism of soliton operation, interaction of solitons and soliton evolution. These findings could provide guidance to the design of desired mode-locked fiber lasers. In the other way, the fundamental soliton in mode-locked fiber lasers becomes unstable when increasing the pump power, complex soliton operation regimes can be observed. In CNT-SA mode-locked fiber lasers, soliton operation and

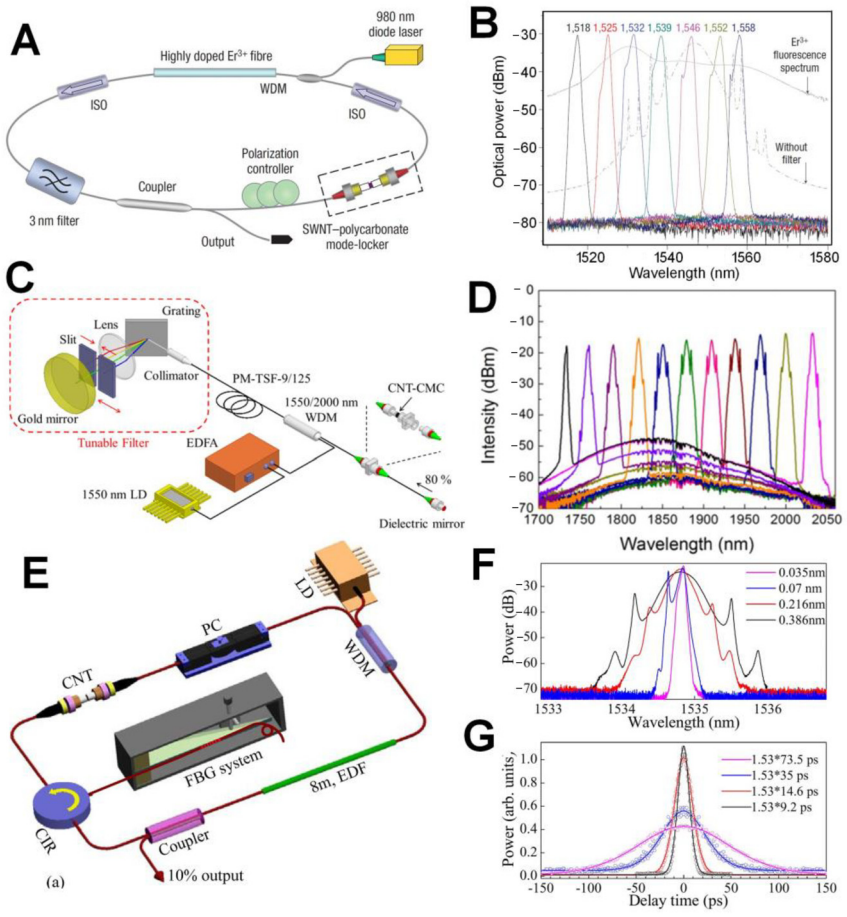

Figure 8: Wavelength and pulse duration tunable CNT-SA mode-locked fiber lasers: (A) 40 nm tunable CNT-SA mode-locked Er-doped fiber laser; (B) Optical spectrum, Wang et al. [37]. © Springer Nature 2008; (C) 300 nm tunable CNT mode-locked Tm-doped fiber laser; (D) Optical spectrum, Dai et al. [65]. © Optical Society of America under the terms of the OSA Open Access Publishing Agreement 2019; (E) Flexible pulse-controlled fiber laser with 7–150 ps pulse duration tunability, (F) Output spectrum; (G) Autocorrelation results, Liu et al. [62]. © Springer Nature 2015.

dynamics, such as the HML, soliton molecule [74, 80, 81, 177], vector solitons [83, 84], dark soliton [85], soliton explosion [178, 179], pulsation [180, 181], and soliton rains [86, 87] have been revealed. Here, we emphasis the dark soliton and soliton rains in CNT-SA mode-locked fiber lasers, others will be discussed in combination with the real-time observations in detail in Section 4. In contrast to the traditional solitons, which are the bright solitons, the dark solitons are a train of pulses with intensity dips inside the continuous wave background [182, 183]. The generation of dark soliton can be explained by the domain wall theory [184, 185]. Generally, large optical nonlinearity is preferred to reduce the pump threshold. Using CNT deposited on the side-polished fiber as the SA, relatively low pump threshold dark pulse and HML dark pulse have been demonstrated. The CNT deposited side-polished fiber could provide saturable absorption and also the large nonlinearity in a short length to reduce the pump threshold [186]. Soliton rains were first reported in 2009 [187], it arouses the researchers' interest due to its unique pulse dynamics that the solitons in the cavity arise from noise background and drift at a constant speed toward a condensed phase like the raindrops generated from the cloud and fall to the sea [188, 189]. The mechanism can be explained by the noise-mediated soliton interaction [190]. Using the advantage of wide working bandwidth of CNT-SA, soliton rains with tunable wavelength (58 nm) have been reported in Tm-doped fiber laser. Vector soliton rains have also been demonstrated [87], and it has an important role in generation of vector bright and dark rouge waves [191].

4 Real-time dynamics of solitons in CNT-based fiber lasers

4.1 Operation principle of TS-DFT technique

The generation of mode-locked pulse is one of the most basic and common nonlinear phenomena in ultrafast fiber lasers. Generally speaking, the mode-locked pulses produced by ultrafast fiber lasers can be called as "optical solitons" due to the balance between dispersion and nonlinear, gain and loss [115]. Although Hasegawa and

Tappert have theoretically predicted that optical fibers could support the transmission of optical solitons as early as 1973 [192], and Mollenauer et al. have firstly confirmed the existence of optical solitons in 1980 [193], the research on solitons in fiber lasers began in the 1990s [194]. Unlike soliton transmission in optical fibers, fiber laser is actually a non-conserved dissipative physical system with periodic gain amplification and output loss. Because of this dissipative characteristic, conventional soliton pulses in fiber lasers will evolve into new soliton states or exhibit complex nonlinear dynamics process under certain conditions. Indeed, a variety of soliton dynamics process has been observed in ultrafast fiber lasers, such as optical rogue waves [195], optical turbulence [196], dissipative soliton resonances [197–201], bound states [202], and a series of other soliton nonlinear phenomena in large dispersion cavity [203, 204]. These results not only further confirm that the ultrafast fiber laser is an ideal platform to explore nonlinear dissipation dynamics, but also deepen the understanding of optical soliton properties.

Nevertheless, these ultrafast nonlinear dissipation dynamics are unrepeatable and have complex transformation in temporal and spectral domain. Due to the limited bandwidth or response speed, the conventional technologies cannot generally measure these rapid nonrepetitive processes. Therefore, many steady state phenomena had been observed theoretically and experimentally, the buildup processes are still unknown. Besides, many interesting and important transient dynamics properties of optical solitons have been theoretically predicted, they are still difficult to be observed and verified experimentally. How to measure these dynamics in real time is a major issue in the field of ultrafast optics. In recent years, the emerging TS-DFT technique has been widely used for real-time, single-shot measurement of the transient, nonrepetitive events [18–20], especially the ultrafast nonlinear optical phenomena. This technique, as a data collection method which can overcome the speed limit of traditional spectrometer, can carry on continuously with billions of frames per second rate and record for trillions of frames. The sampling rate is about 10 orders of magnitude higher than the conventional spectrometer. This technique opens up the way for experimental measurement and understanding the behavior of ultrafast non-stationary and rare phenomena in complex nonlinear system. So far, TS-DFT technique has gained intense attentions from optical sensing [205], spectroscopy [206], optical imaging [207], biomedicine [208], and other fields [209]. Using TS-DFT technique, lots of transient dynamics of soliton in the mode-locking fiber laser have been revealed and demonstrated experimentally, including entire buildup dynamics of solitons, soliton molecules, soliton explosion and so on.

The TS-DFT technique derives from the analogy between spatial Fraunhofer diffraction and temporal dispersion, in which the diffraction of a beam through a lens in the far-field region is analogous to the propagation of a time pulse in a dispersion medium, also known as the space–time duality [21]. As shown in Figure 9, when a soliton is propagating along the dispersive element with enough dispersion to satisfy the time far-field condition, it is stretched due to the group velocity dispersion (GVD), different wavelengths in the spectrum are mapped into temporal domain, and the stretched light pulse has the same intensity envelope as the spectrum shape, thus realizing spectrum detection of targeting pulses in temporal domain. Ultimately, single-shot spectrum information can be detected by using high-speed analog digital converter (ADC). It should be noted that this technique is usually viable for shorter pulses measurement (e. g., less than 10 ps), continuous wave and longer pulses measurement (e. g., more than 20 ps) that corresponds to a narrow spectral width are usually unviable [74]. Compared with traditional spectrometers, TS-DFT technique has another advantage: its dispersion medium can also be used as an incremental medium for optical amplification [18, 210]. By conducting distributed amplification of light pulses in dispersion fiber, the trade-off between sensitivity, speed, and resolution in spectral measurement can be overcome [20].

There are several kinds of dispersive elements for implementing time-stretch system, such as single-mode fiber (SMF), dispersion compensated fiber (DCF), CFBG, multimode waveguide and so on [211–214]. These dispersive elements can generate both linear dispersion for conventional time stretch and nonlinear dispersion for warped (foveated) stretch. The latter has been used for optical data compression via non-uniform Fourier domain sampling, whereby information-rich portions of the

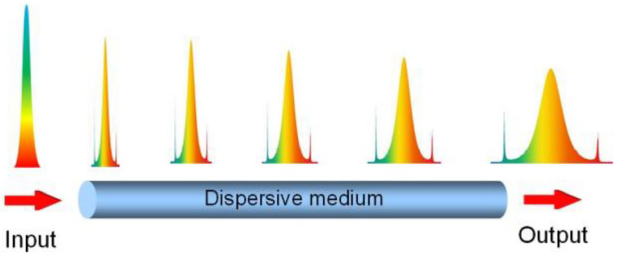

Figure 9: Schematic diagram of TS-DFT technique. The ultrashort pulses are stretched and mapped into the temporal domain through enough dispersion.

spectrum are sampled at a higher density than sparse regions, leading to the concept of the analog information gearbox. For Tm-doped fiber laser with operating wavelength around 2 μm, the CFBG is usually adopted to surmount the high transmission loss of general fiber [215]. Using TS-DFT technique, lots of transient dynamics of soliton in the mode-locking fiber laser have been revealed and demonstrated experimentally, including entire buildup dynamics of solitons, soliton molecules, soliton explosion and so on.

4.2 Entire formation dynamics of solitons

4.2.1 Buildup dynamics of mode-locking soliton

Mode-locking, as a complex nonlinear phenomenon in lasers, can lock a large number of laser longitudinal modes together in the cavity to form ultrashort pulses. Despite the stable pulse train formed through mode-locking, the initial buildup process of pulses is highly random and non-repetitive [5, 220]. Since the 1990s, the nonlinear dynamics of mode-locked lasers has been reported by researchers through a large number of experiments and theories, with the emphasis being on self-starting [221–226]. In the stationary state, the soliton train generated from mode-locked lasers can be described theoretically by means of the generalized nonlinear Schrödinger equation (GNLSE) or the Ginzburg–Landau equation (GLE) [17], many interesting phenomena and soliton operation had been reported in a variety of laser configurations. However, due to the limitations of instrument scanning rate and bandwidth, the experimental study on the transient process established by mode-locking mainly relies on high-speed oscilloscopes to observe the pulse dynamics in temporal domain, the corresponding real-time spectral evolution characteristics have not been experimentally studied.

Recently, with the rapid development of real-time measurement technique, researchers have used TS-DFT technique to reveal many dynamics processes in mode-locked ultrafast lasers. As an important nonlinear phenomenon, the study of the soliton transient dynamics has naturally aroused the interests of relevant researchers. Therefore, both the transient spectral and temporal dynamics were observed with the assistance of the TS-DFT technique. In 2016, Herink et al. used the TS-DFT technique to firstly study and analyze the transient process of solitons in Kerr-lens mode-locking Ti:sapphire laser, they observed the interesting phenomenon of spectral transient interference pattern prior to the stable soliton train, which is also known as beating dynamics [219]. As shown in Figure 10(D), the long-recording-length consecutive shot-to-shot spectrum evolution dynamics revealed the birth of mode-locking pulse from the initial fluctuations, together with wavelength shifts. However, the formation process of mode-locking pulse in fiber lasers is still unknown. By combing with the TS-DFT and time lens techniques, Dudley et al. completely unveiled the spectral and temporal evolution of dissipative solitons in a passively mode-locking fiber laser based on SA mirror, showing that solitons will pass through a transient unstable regime with complex break-up and collisions before stabilization [217]. More recently, Zeng et al. unveiled the buildup dynamics of dissipative solitons in NPR based mode-locked fiber lasers by means of the TS-DFT technique, showing that the role of initial noise background is to stimulate modulation instability [218]. They observed two paths of dissipative soliton buildup dynamics, depending on the length of the laser cavity. In a long cavity, multiple processes are involved in the buildup phase, including modulation instability (Benjamin–Feir instability), mode locking, self-phase modulation (SPM)-induced instability, dissipative soliton splitting, and partial annihilation. In a short cavity, only modulation instability and mode locking are responsible for dissipative soliton formation. A long-standing issue in the buildup of mode locking refers to the role of noise involved: a randomly strong noise spike was assumed to evolve into mode-locked pulse [5].

However, in all previous works, the mode-locking technique is quite sensitive to environmental perturbations (e. g., the polarization changes in laser cavity and the fluctuation of pumping strength). Therefore, pulses generated from these fiber lasers will sustain extra unstable stages, such as Q-switched lasing [228–230]. Moreover, relaxation oscillations (ROs), which have been predicted in fiber laser [231], were excluded from their reports. To reveal the entire buildup process of solitons, we must mitigate the environmental perturbation as far as possible. CNTs have the advantages of high stability and polarization independence. Using CNTs as SA can greatly reduce the sensitivity of buildup process to environmental perturbations, inhibit Q-switched lasing, make the buildup of solitons return to the real process and shorten the starting time.

In 2018, Luo et al. experimentally observed the buildup dynamics of dissipative soliton in an ultrafast fiber laser in the net-normal dispersion regime [232] and conventional soliton booting dynamics of an ultrafast fiber laser operating in an anomalous dispersion regime [233]. They firstly revealed that the appearance of the spectral sharp peaks with oscillation structures during the mode-locking transition is caused by the formation of structural dissipative

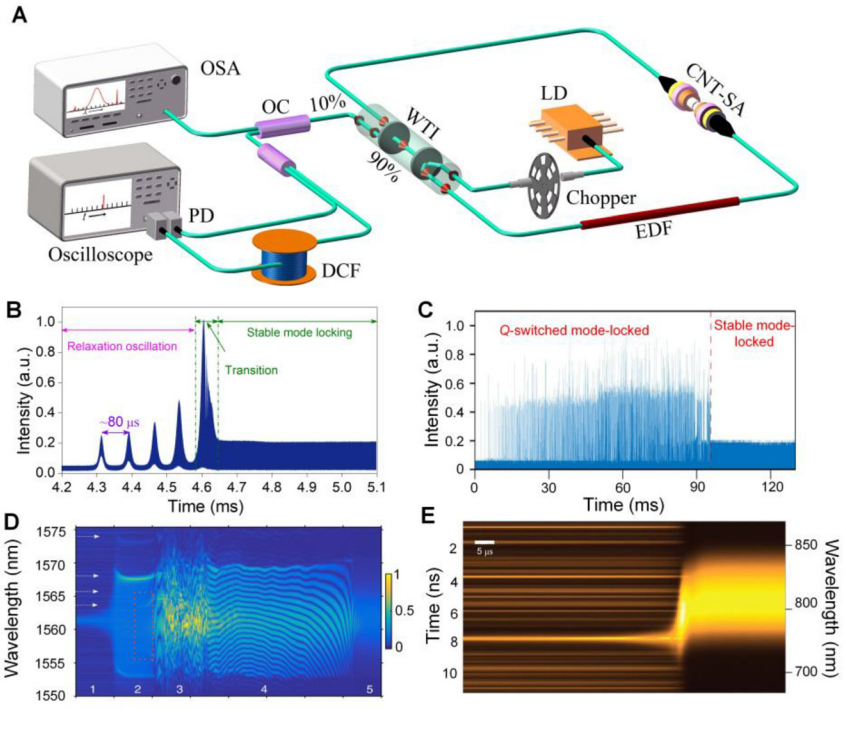

Figure 10: Experimental real-time measurement of the buildup dynamics of solitons based on various mode-locking techniques: (A) A typical schematic diagram of conducting ultrafast measurement of mode-locked lasers based on TS-DFT, Liu et al. [74] © American Physical Society 2018; (B) CNT-based saturable absorber, Liu et al. [216]. © SPIE 2019; (C) Saturable absorber mirror (SA-M), Ryczkowski et al. [217]. © Macmillan Publishers Limited 2018; (D) Nonlinear polarization rotation (NPR), Peng et al. [218]. © Springer Nature Limited 2018; (E) Kerr-lens Ti:sapphire, Herink et al. [219]. © Macmillan Publishers Limited 2016. In (D) and (E), the two-dimensional representations are achieved through segmenting the time series into intervals of roundtrip time, the vertical and horizontal axes depict the information within a single roundtrip and the dynamics across consecutive roundtrips, respectively.

soliton. In 2019, Liu et al. demonstrate the first observation of the entire buildup process of conventional solitons in a mode-locked laser in the net-anomalous dispersion regime, revealing two possible pathways to generate the temporal solitons by optimizing the laser system to improve its stability, which suppresses the Q-switched lasing induced by environmental perturbation [216]. One pathway includes the dynamics of raised RO, quasi mode-locking stage, spectral beating behavior, and finally the stable single-soliton mode-locking, as shown in Figure 11(A). The other pathway contains, however, an extra transient bound-state stage before the final single-pulse mode- locking operation, as shown in Figure 11(C). Moreover, the complete evolution dynamics (from birth to extinction) of the CS, StP, and DS are also investigated by using the DFT technique [227]. CS, StP, and DS fiber lasers mode locked by SWCNT-SA are implemented via engineering the intracavity dispersion map. The RO can always be observed prior to the formation of stable soliton operation due to the inherent advantage of SWCNT, but it exhibits distinct evolution dynamics in the starting and shutting processes. The shutting processes are dependent on the dispersion condition and turn-off time, which is against common sense. Some critical phenomena are also observed, including transient complex spectrum broadening and frequency-shift interaction of SPs and picosecond pulses. More recently, Kudelin et al. experimentally demonstrated that bidirectional soliton fiber laser experience independent buildup dynamics from modulation instability, undergoing breathing dynamics and diverging sub-ordinate pulse structures formation and annihilation [234]. In the same way, the similar behaviors dissipative soliton in a net-normal-dispersion bidirectional ultrafast fiber laser were also observed by Luo et al. [235].

In addition, Q-switching (QS) is also another way used for pulse generation which is based on the modulation of the quality factor (Q) of a laser cavity. This method enables the formation of pulses with durations ranging from micro- to nanoseconds and repetition rates, typically around kilohertz, related to the lifetime of the gain medium [95]. Recently, we reported the first observation of pulse evolution and dynamics in the QS-ML transition stage, as shown in Figure 12, where the ML soliton formation evolves from the QS pulses instead of ROs (or quasi-continuous-wave oscillations) reported in previous studies [73]. We discovered a new way of soliton buildup in an ultrafast laser, passing through four stages: initial spontaneous noise, QS, beating dynamics, and final stable ML. The research on the entire buildup of mode-locking soliton can provide guidance to design and optimization of highly performance mode-locked fiber lasers, as well as promote the application of ultrafast fiber lasers.

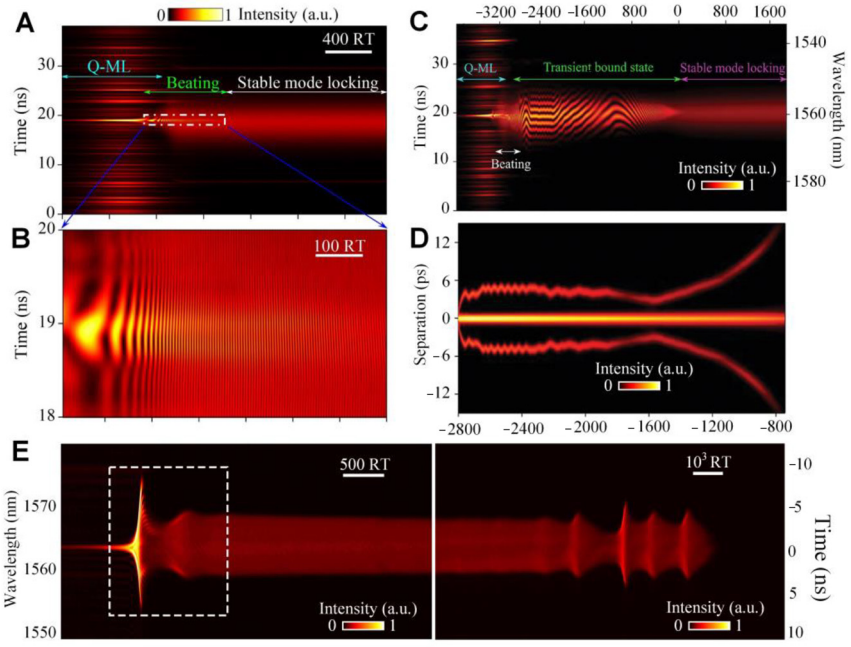

Figure 11: Entire buildup dynamics of conventional soliton and dissipative soliton. (A, B) Formation dynamics of single soliton with beating dynamics; (C, D) Buildup dynamics of single soliton with transient bound state. Liu et al. [216]. © SPIE 2019; (E) Formation and extinction dynamics of dissipative soliton. Cui et al. [227]. © Chinese Laser Press 2019.

4.2.2 Buildup dynamics of soliton molecules

As we know, when the pump power is high in the cavity, it often leads to the generation of multiple pulses. However, the interaction between solitons will cause multiple solitons to be rearranged, thus forming a variety of "multiple soliton patterns", such as soliton molecules (SMs), soliton beams, and soliton rains [238, 239]. SMs, as one of the most fascinating nonlinear phenomena, have been a hot topic in the field of nonlinear optics in recent years. SMs can form or dissociate in various isomers, considering the relative temporal separation and phase difference between adjacent pulses as internal dynamical degrees of freedom [240]. In 2017, Herink et al. firstly resolved the evolution of femtosecond soliton molecules in the cavity of a few-cycle mode-locked laser [236]. They have tracked two- and three-soliton bound states over hundreds of thousands of consecutive cavity roundtrips, identifying fixed points, and periodic and aperiodic molecular orbits. In 2018, Grelu et al. presented the first direct experimental evidence of the internal motion of a dissipative optical SM generated in a passively mode-locked fiber laser. They map the internal motion of a soliton pair molecule by using a dispersive Fourier-transform imaging technique, revealing different categories of internal pulsations, including vibration like and phase drifting dynamics [241]. Later on, Liu et al. experimentally observed several types of evolving SMs with monotonically or chaotically evolving phase, flipping

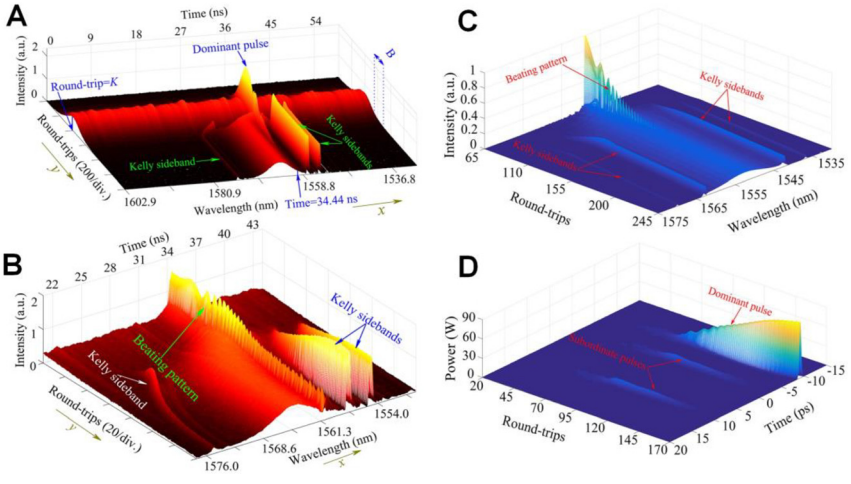

Figure 12: Spectral evolution dynamics of soliton in the QS-ML transition stage. (A, B) Real-time observation results by TS-DFT technique. (C, D) Numerical simulation results with beating dynamics. Liu et al. [73]. © American Physical Society 2019.

and hopping phase in an ultrafast fiber laser by using the TS-DFT technique [242]. Moreover, a shaking SM has also been experimentally observed [243]. Beyond the simplex vibrating soliton pairs, multiple oscillatory motions can jointly involve during the internal dynamics, reminiscent of the shaking soliton pairs. In addition, the shaking soliton pair combined with sliding phase dynamics was also observed, it was interpreted as the superposition of two different internal motions. Furthermore, Peng et al. described the formation of another three types of SMs: ground- and excited-state SMs (corresponding to the close- and wide-separation solitons, respectively), as well as a newly termed intermittent-vibration SM [237]. They found that the formations of all these SMs consist of three nonlinear stages: mode locking, soliton splitting, and soliton interactions. Moreover, they have reported on the direct experimental observation of breathing dissipative SMs in a passively mode-locked fiber laser [244]. By using CFBGs, the similar internal motions within dissipative optical SMs in the 2 μm wavelength range have also been reported [215].

Nevertheless, due to the environmental perturbations of these mode-locking mechanisms, the entire buildup process of stable long-lived SMs, which is similar with that of single soliton, has not been reported. By decreasing external perturbations, optimizing the laser system and using the SWCNT as mode-locker, we successfully tracked the formation and evolution of SMs, showing that the birth dynamics of a stable SM experiences five different stages, i. e., the raised RO stage, beating dynamics stage, transient single pulse stage, transient bound state, and finally the stable bound state [74], as shown in Figure 13(A). We discovered that the evolution of pulses in the raised RO stage follows a law that only the strongest one can ultimately survive. Meanwhile, the pulses periodically appear at the same temporal positions for all lasing spikes during the same RO stage (named as memory ability) but they lose such ability between different RO stages. The existence of an RO stage is a typical characteristic of the transient behavior of lasers [231, 245]. The experimental observation demonstrated that multiple sub-nanosecond pulses appear in the RO stage but only one dominant pulse gradually evolved into the stationary mode-locking soliton.

Soliton self-organization is another dynamic process in which many solitons interact to form soliton molecules. According to the different mechanism of action, these bound states have different intensity, phase, and spacing. It is important to observe the soliton interaction process in real-time to understand the dissipative soliton self-organization process. In 2018, Wang et al. observed the dynamics soliton self-organization and pulsation in passively mode-locked fiber laser. Due to the acousto-optic effect, the solitons can mix and form evenly spaced soliton

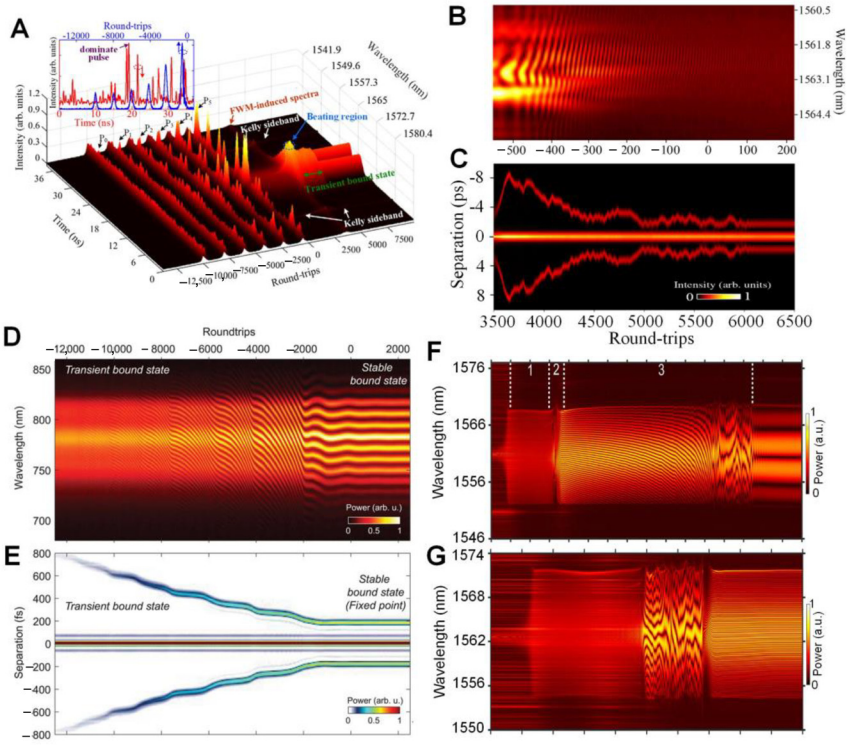

Figure 13: Various formation and evolution dynamics of soliton molecules. (A–C) Entire formation dynamics of soliton molecules in CNT-based fiber laser. Liu et al. [74]. © American Physical Society 2018; (D, E) Formation of a soliton molecule from transient bound state. Herink et al. [236]. © American Association for the Advancement of Science 2017; (F) Formation dynamics of ground-state soliton molecule; (G) Buildup dynamics of excited-state soliton molecule. Peng et al. [237]. © WILEY-VCH Verlag GmbH & Co. KGaA, Weinheim 2018.

bunches. By using the TS-DFT technique, they found the spacing of solitons in one bunch is different, while their phase relation is fixed. Soliton pulsation was also observed, and Kelly sideband appeared with the pulsating period [246]. The study on the dynamics of soliton molecule brings new perspectives for ultrafast transient dynamics and opens new pathways of pulses evolution and interaction that will reveal the physics of solitons dynamics in nonlinear system.

4.2.3 Buildup dynamics of harmonic mode-locking soliton

As mentioned in Section 3, passive HML is an effective method to increase the pulse repetition rates of fiber lasers, it has the intrinsic advantage of repetition-rate self-stabilization. Harmonically mode-locked fiber laser can be realized through active mode-locking [247, 248], passive mode-locking [249, 250], and hybrid mode-locking [251, 252]. However, the problem of how harmonics are generated and the mechanism by which self-stability is achieved has plagued researchers for many years. The solution to these problems can provide great guidance value for the design and implementation of harmonic lasers. Generally, the spacing between multiple pulses operated in HML undergoes a random change due to the presence of temperature variations and mechanical vibrations. As a result, the HML operation in the ordinary non-polarization-maintaining (non-PM) fiber lasers can only remain stable in a short time-scale, and even such operation is discontinued by these perturbations. The controllable HML operation of passively mode-locked fiber lasers, on the other hand, has been proved quite hard to be achieved. Coupling between cavity modes and the acoustic resonance in a fiber provides strong and optomechanical interactions, resulting in "control elements" that enable controllable and stable HML operation of lasers. More recently, passive harmonic mode-locking of fiber laser using CNT-SA was also reported for environmentally stable and self-starting operation compared to the NPE method [82, 168, 253].

Based on the TS-DFT technique, combined with the specially designed full polarization-maintaining optical cavity, we conducted a detailed experimental study on the formation dynamics in SWCNT-SA passive HML laser [75], as shown in Figure 14(C). The results demonstrated that the buildup process of HML includes such stages as the raised RO, beating dynamics, birth of a giant pulse, self-phase modulation (SPM)-induced instability, pulse splitting, repulsion and separation of multiple pulses, and the stable HML state. It was observed that the multiple HML pulses originate from a single-pulse splitting phenomenon and a remarkable breathing behavior occurs at an early stage of the HML buildup process. Furthermore, the HML pulses are found originating from a giant pulse whose temporal evolution trajectory shows a turning point (or a big corner) as a consequence of intensity reduction induced pulse group velocity change. While for a short-cavity laser configuration involving a SESAM [254], HML soliton were observed to be generated from a transient multi-pulse state rather than a giant pulse as shown in Figure 14(A). Our numerical results confirm that the effects of dispersive wave [255], gain depletion and recovery [256, 257], and acoustic wave [258, 259] play key roles in the earlier, middle, and later stages of this HML buildup process, respectively; as well, the acoustic resonance in the single-mode fiber stabilizes the final HML state of lasers. By means of the optoacoustic effect that induces a trapping potential, the acoustic resonance can stabilize the mode-locking of laser at different harmonics (from the first to sixth order at the appropriate pumping strength) with perfect long-term stability. The study of the entire buildup dynamics of HML can bring insight into the complex nonlinear system and provide guidance to the design of ultrahigh repetition rate fiber lasers. These results can also bring new perspectives into the transient dynamics of ultrafast phenomena and helps to understand the dynamics of nonlinear system.

4.2.4 Buildup dynamics of multi-solitons

In addition to stable pulse generation, passively mode-locked fiber lasers can easily run into an unstable regime of multi-pulse mode-locking [261, 262]. Several theoretical attempts have been made to interpret the mechanism behind multi-pulse mode-locking, e. g., peak power clamping [263], gain bandwidth limited pulse splitting [264], and nonlinear cavity feedback [265]. In terms of experimental investigations, however, it is seriously limited by the poor temporal resolution of conventional spectroscopic techniques, which thus hinders the spectral-temporal study of individual pulses. Therefore, tracking the behavior of a single pulse within the multi-pulse cluster has been mostly conducted by numerical simulations and temporal observation [266]. The birth and dynamic behaviors of multi-pulse mode-locking so far have rarely been experimentally explored, particularly in the spectral domain. In 2017, Yu et al. reported several kinds of multi-pulse spectral-temporal dynamics of a passively mode-locked fiber laser observed in a single-shot manner, e. g.,

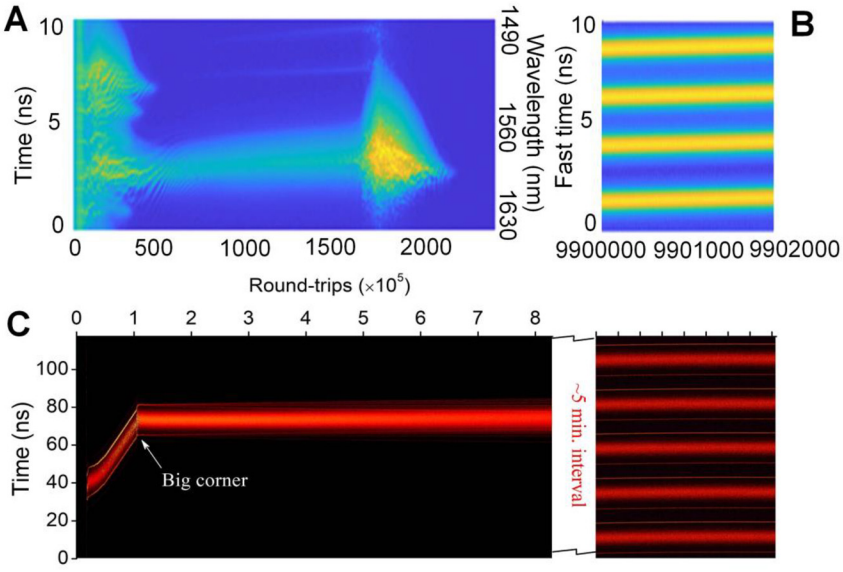

Figure 14: Entire formation dynamics of HML in a passively mode-locked laser with (A, B) short-cavity based on semiconductor SA mirror. Wang et al. [254]. © Optical Society of America 2019; (C) long-cavity based on CNT-SA. Liu et al. [75]. © WILEY-VCH Verlag GmbH & Co. KGaA, Weinheim 2019.

energy quantization, self-phase modulation spectral broadening, wavelength shifting, spectral interfering, and ultraweak pulse interaction [260], as shown in Figure 15(A) and (B). In addition, they also studied the intracavity collision process induced by dual-color in a mode-locked fiber laser [267]. In 2018, Wang et al. studied the double pulse evolution process of the transient loss of lock [268], they found that the double pulse can disappear at the same time or one by one. It is worth noting that the decline rate of pump power has a significant impact on the lose process of the bound state. These findings contribute to a better understanding of soliton dynamics characteristics of the mode-locked fiber laser. However, the multi-soliton states mentioned above are generated synchronously in the laser cavity. Recently, we report the real-time experimental observation of asynchronous multi-soliton buildup dynamics in all-polarization-maintaining mode-locked fiber laser [269], as shown in Figure 15(C)–(D). The solitons are generated one by one from soliton shaping of distant background pulses under independent processes; each is the result of a separate beating dynamics. Resonant energy transfer between dispersive waves and background pulses is observed. With the birth of the last soliton, the solitons are stable and exhibit energy quantization properties. More recently, Zeng et al. also demonstrated that an additional soliton is formed through shaping of a narrow-band pulse arising from a dispersive wave (DW), thus differing from pulse splitting processes that originated from a single pulse [270]. These results can provide novel prospective into the multi-soliton buildup dynamics, interaction and regulation in mode-locked lasers.

4.3 Localized transient dynamics of solitons

4.3.1 Soliton pulsation dynamics

Generally speaking, when the pulses output from a certain point of the laser cavity, they would have the same characteristic and do not change with time, that is the stable operating state of the laser. However, in some conditions, the soliton pulsation can be observed, in which the profile, width and amplitude of the output pulses change periodically by altering the nonlinear gain absorption or spectral filtering effect of the laser [271–273]. In 2018, Wei et al. demonstrated the chaotic soliton pulsation and the stable molecular state of the soliton in a passively mode-locking fiber laser by using the TS-DFT technology [274]. In the chaotic soliton pulsation, the periodic soliton would undergo a sudden collapse and recovery process similar to the soliton explosion. Although most research on motion of solitons is conducted in anomalous dispersion region, this phenomenon can also occur in the normal dispersion region. In 2018, Du et al. observed the dissipative soliton pulsation process in the normal dispersion mode-locked fiber laser and studied the spectral respiration effect in the pulsation process based on the TS-DFT technology [275]. Recently, Luo et al. reported a new type of soliton pulsation in the context of ultrafast fiber lasers and visualized it by the DFT technique. This type of soliton pulsation features that shot-to-shot spectra evolve with roundtrips, but the pulse energy remains almost unchanged, which is termed as “invisible soliton pulsation”. Different pulsating periods were also obtained by properly adjusting of cavity

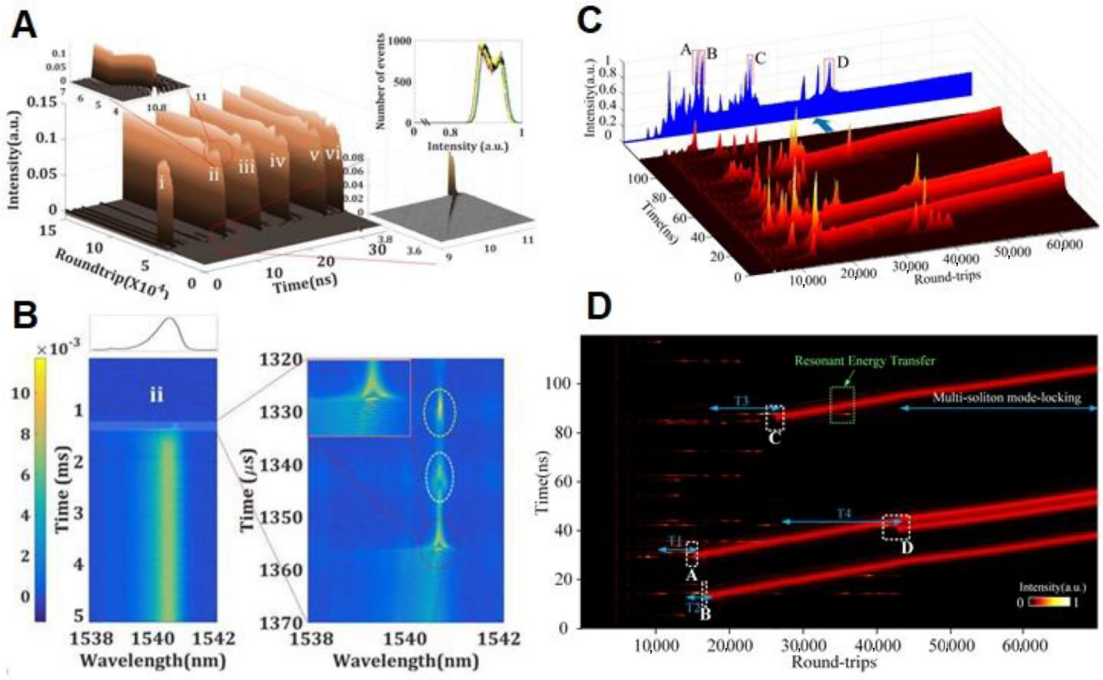

Figure 15: Multi-soliton buildup dynamics with different ways. (A, B) Synchronous generation. Yu et al. [260]. © American Institute of Physics 2017; (C, D) Asynchronous formation.

parameters, i. e., pump power and polarization controller (PC), demonstrating that the invisible soliton pulsation could exist in a range of cavity parameters, rather than a rare phenomenon [276].

More recently, Xu et al. revealed the distinct dynamical diversity of pulsating solitons in a fiber laser by using hybrid mode-locking based on NPR and CNT-SA [180], as shown in Figure 16(A)–(B). In particular, the weak to strong explosive behaviors of pulsating solitons, as well as the rogue wave generation during explosions were observed. Moreover, the concept of soliton pulsation is extended to the multi-soliton regime. It was found that the simultaneous pulsations of energy, separation and relative phase difference could be observed for solitons inside the molecule, while the pulsations of each individual soliton in a multi-soliton bunch could be regular or irregular. These studies can provide new insights into the complex nonlinear system and contribute to the design of fiber lasers for practical applications.

4.3.2 Vector soliton dynamics

During the forming of the soliton in fiber laser, since single-mode fiber has weak birefringence due to the non-perfect cylindrical symmetry of the fiber or externally applied random stress to the fiber, the laser can support vector soliton [277–279]. Vector soliton can be formed in mode-locked fiber laser that is insensitive to polarization [280, 281]. The phase and intensity of two orthogonal components depend on the net cavity birefringence and coupling strength, which can be classified as polarization locked vector solitons (PLVS), polarization rotation vector solitons (PRVS), group-velocity locked vector solitons (GVLVS) and so on [83, 84, 181, 279–281]. Among them, the intensity of the two orthogonally polarized components of the PRVS will change alternately, so the corresponding spectrum will also change with it. However, due to the limited performance of spectrometer, this change was not observed in the experiment. In 2017, Krupa et al. studied coherent vector spectrum evolution dynamics characteristics of dissipative soliton in SESAM mode-locked fiber laser by using the TS-DFT technique [282]. They observed the polarization locking and polarization switching effects of the incoherent soliton, found the vector soliton can be locked in one polarization or jump between the two-polarization cycles. Recently, Luo et al. experimentally observed the real-time spectral characteristics of the polarization components of the GLVS and PLVS by using TS-DFT technique, they revealed the dynamical capturing characteristics of the soliton for the first time [181], as shown in Figure 16(C)–(D). For the GLVS, the central wavelength of its two-polarization components remains unchanged,

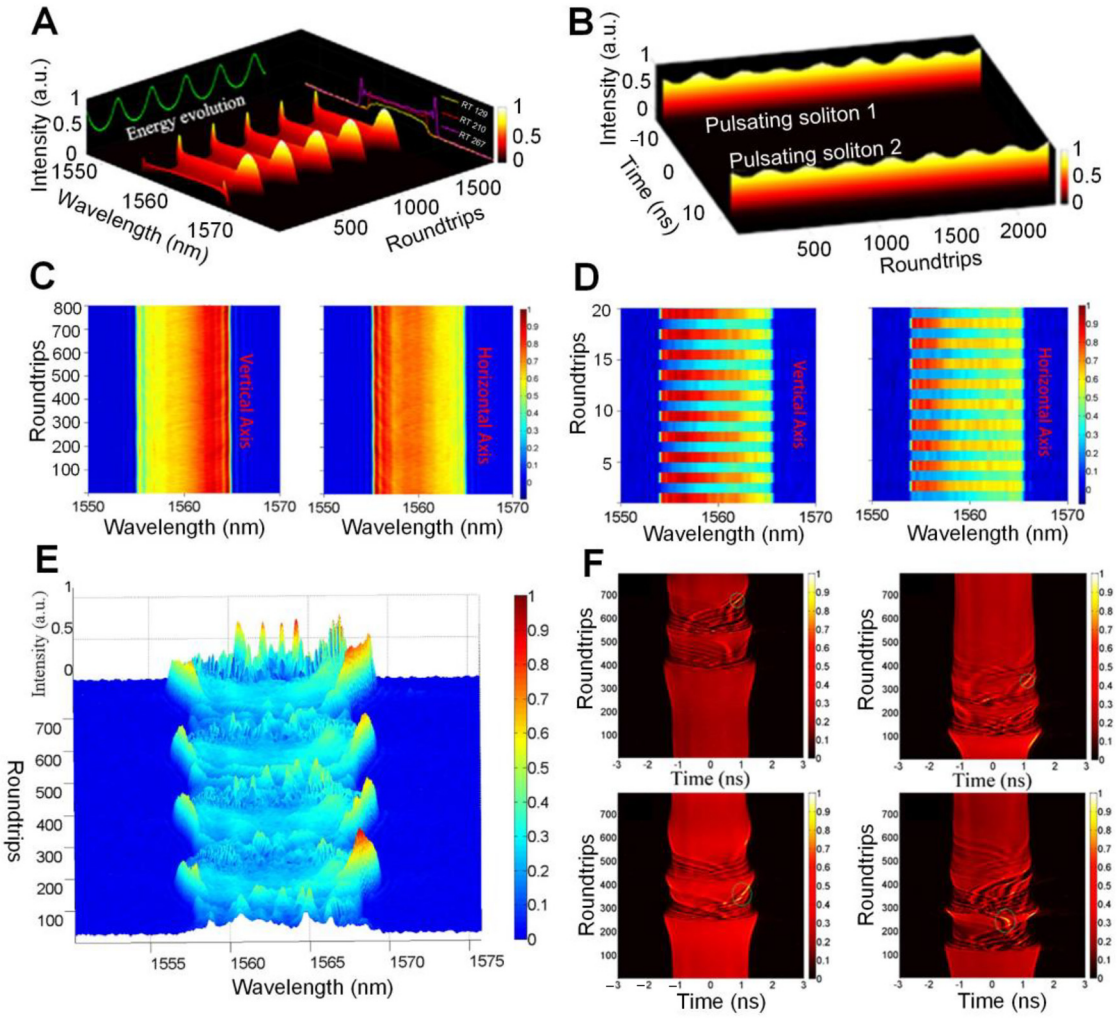

Figure 16: Various steady-state dynamics of soliton. (A) Single-shot spectra and corresponding energy evolution dynamics of single-soliton pulsation; (B) Single-shot spectra evolution of single-soliton pulsation; Xu et al. [180]. © Optical Society of America 2019. (C) Single-shot spectra evolution dynamics of GLVS. (D) Single-shot spectra evolution dynamics of PRVS. Liu et al. [181]. © Optical Society of America 2017. (E) Shot-to-shot spectra in "successive soliton explosions" regime. Liu et al. [178]. © Optical Society of America 2016. (F) Spectral evolution dynamics of four typical single-shot pulse-trains in soliton explosion regime. Liu et al. [179]. © Optical Society of America 2016.

while the PLVS's two polarization components are trapped by changing the central wavelength dynamically. Recently, Cui et al. reported on the observation of a cross-phase-modulation-forced frequency-oscillating soliton whose wavelength exhibits redshift and blueshift periodically like dancing in a mode-locked fiber laser under moderate birefringence [283]. Cao et al. demonstrate a novel polarization-dependent pulse dynamic in a fiber laser cavity mode-locked by single-wall CNTs. By managing the net dispersion and polarization state, they obtained two noise-like pulsing procedures with distinctive polarization characteristics together with coherent energy coupling between pulses during the switching process [284]. These results can reveal the complex nonlinear dynamics of soliton dynamics and promote the research of complex transient phenomena in nonlinear system.

4.3.3 Soliton explosion and optical rogue wave

Because of the self-organizing effect of the dissipative system, the laser can operate in stable, quasi-stable and non-stable states. Soliton explosion, as one of the most interesting nonlinear phenomena in quasi-steady state, has also recently attracted extensive attention from relevant researchers [271, 272, 285]. A typical feature of a soliton explosion is that a quasi-stationary pulse suddenly experiences a structural collapse as it travels back and forth through the cavity, but after a sustained period of

operation, the collapsed pulse returns to its original intact state. As early as 2002, Cundiff et al. demonstrated the existence of the soliton explosion [286] in a mode-locked Kerr-lens Ti:sapphire laser. However due to the lack of high-resolution real-time measurement tools, more details of this transient phenomenon remain to be revealed. In 2015, Runge et al. first observed the transient spectral characteristics of soliton explosion in a fiber laser by using TS-DFT technique [287, 288]. In 2019, Zeng et al. reported on experimental observation of breathing DS explosions in mode-locked fiber lasers. A bifurcation diagram clearly showed how the different laser regimes, including breathing DS explosions, breathing DSs, and continuous-wave mode locking, can be switched by varying the pump power. While soliton explosions are found above the pump power for generating stable solitons, breathing DS explosions occur under the pump power for generating stable breathing DSs [289].

The evolution of the optical spectrum in the stage of soliton explosion can be studied by using TS-DFT technique, which is of great significance for the analysis of the underlying mechanism. In 2016, Liu et al. studied the dissipated rogue wave phenomenon caused by the soliton explosion [179], as shown in Figure 16(F). By statistically analyzing of the pulse energy recorded by TS-DFT technique during the soliton explosion, they found that the phenomenon was accompanied by rogue waves during the explosion. In 2018, Luo et al. reported on the soliton dynamics of an ultrafast fiber laser from steady state to soliton explosions and to huge explosions by simply adjusting the pump power level. In particular, the huge soliton explosions show that the exploding behavior could operate in a sustained, but periodic, mode from one explosion to another, which they termed as “successive soliton explosions” [178], as shown in Figure 16(E). In 2018, Yu et al. observed the soliton explosion in a mode-locked multi-soliton laser and found that the explosion of a soliton would cause the explosion of other solitons through the interaction of gain. This phenomenon is known as mutually ignited soliton explosions [290]. As one of the most striking nonlinear dissipative phenomena in ultrafast lasers, these studies can bring new insight into the dynamics of soliton explosion and rouge waves and promote the deep understanding of the ultrafast lasers.

5 Conclusion and outlook

In summary, we have reviewed the recent progress in the dynamics of CNT-SA ultrafast fiber lasers, with emphasis on recent progress in real-time buildup dynamics of solitons in CNT-SA mode-locking fiber lasers. The successful application of CNT as SA has promoted the development of scientific research of ultrafast fiber lasers. Its excellent properties have enabled ultra-stable and compact fiber laser system with ultrashort and high energy pulse output covering the visible to the mid-infrared spectral region. Various pulse evolution and interaction dynamics were revealed based on CNT-SA mode-locked fiber lasers, and various functions were achieved to meet practical application requirement of multiple fields. Besides, the CNT-SA mode-locked fiber laser can provide an excellent platform for investigating the entire formation and steady-state dynamics of solitons and other nonlinear phenomena. By using the emerging TS-DFT technique, many kinds of soliton dynamics phenomenon including mode-locking soliton, soliton molecules, multi-soliton, and soliton explosions were unveiled based on the CNT-SA mode-locked fiber laser, the results provided a variety of dissipative dynamics process evolution details. These studies will promote the development of ultrafast lasers, help to understand the physical nature of solitons and also provide references for the interpretation of dissipative soliton phenomena in other fields.

At present, the real-time observation of time-domain characteristics of ultrafast dynamics mainly depends on high-speed oscilloscope. For the existing oscilloscopes, time resolution and record length have irreconcilable contradictions. Real-time measurements of pulse intensity with sub-picosecond time resolution and long recorded lengths are essential for a comprehensive understanding and further study of the various slowly evolving ultrafast dynamics. Recently, researchers have proposed the use of time-lens based on the duality of space-time to study the real-time waveform evolution characteristics of ultrafast nonlinear phenomena [291, 292]. This time-lens technique has been applied to the study of incoherent soliton transmission in optical turbulence [293, 294] and the occurrence of random breathing in modulation instability. In the study of transient dynamics of solitons in ultra-fast fiber lasers, researchers combined TS-DFT technique with time lens technology to observe the spectra and time characteristics of transient processes established by solitons in real time [228] and other nonlinear phenomena, such as Turing and Faraday instabilities [295]. Moreover, together with emerging intelligent algorithm, the TS-DFT technique can make mode-locking fiber laser more portable and spectrum-programmable [296]. We believe that this multi-scale real-time measurement technique will contribute to a more comprehensive understanding of soliton transient dynamics in ultrafast fiber lasers, such as mode-locking startup, soliton explosion, and rogue waves. The study on

transient dynamics of soliton in ultrafast fiber lasers by using TS-DFT technology breaks the limitation of experimental observation of ultrafast phenomena by traditional electronic measuring instruments and greatly inspires researchers to continue to explore new nonlinear phenomena of soliton. We believe that the study of transient dynamics of solitons can not only further reveal the physical nature of solitons, but also optimize the performance of ultrafast fiber lasers and eventually expand their applications in different fields. Meanwhile, as a typical nonlinear system, the performance improvement of fiber laser can also provide a better test platform for the exploration of soliton nonlinear phenomena.

Acknowledgments: This work was supported by the National Natural Science Foundation of China under Grants No. 61525505 and No. 11774310, and the Postdoctoral Science Foundation of China under Grants No. 2019M652076.
Author contributions: All authors have accepted responsibility for the entire content of this manuscript and approved its submission.
Research funding: None declared.
Competing interests: Authors state no conflict of interest.

References

[1] M. E. Fermann and I. Hartl, "Ultrafast fibre lasers," *Nat. Photonics*, vol. 7, pp. 868–874, 2013.
[2] F. W. Wise, A. Chong, and W. H. Renninger, "High-energy femtosecond fiber lasers based on pulse propagation at normal dispersion," *Laser Photon Rev.*, vol. 2, pp. 58–73, 2008.
[3] N. J. Doran and D. Wood. "Nonlinear-optical loop mirror," *Opt. Lett.*, vol. 13, pp. 56–58, 1988.
[4] F. X. Kartner, I. D. Jung, and U. Keller. "Soliton mode-locking with saturable absorbers," *IEEE J. Sel. Top Quantum Electron.*, vol. 2, pp. 540–556, 1996.
[5] U. Keller, "Recent developments in compact ultrafast lasers," *Nature*, vol. 424, pp. 831–838, 2003.
[6] A. E. Siegman. *Lasers University Science Books*. CA, Mill Val, 1986.
[7] A. Martinez and Z. Sun, "Nanotube and graphene saturable absorbers for fibre lasers," *Nat. Photonics* 2013, vol. 7, pp. 842–845.
[8] S. Y. Set, H. Yaguchi, and Y. Tanaka, et al., "Mode-locked fiber lasers based on a saturable absorber incorporating carbon nanotubes," in *Optical Fiber Communication Conference, Optical Society of America*, 2003, p. PD44.
[9] V. Scardaci, Z. Sun, F. Wang, et al., "Carbon nanotube polycarbonate composites for ultrafast lasers," *Adv. Mater.*, vol. 20, pp. 4040–4043, 2008.
[10] J. Wang, Y. Chen, and W. J. Blau, "Carbon nanotubes and nanotube composites for nonlinear optical devices," *J. Mater. Chem.*, vol. 19, pp. 7425–7443, 2009.
[11] Z. Sun, T. Hasan, and A. C. Ferrari, "Ultrafast lasers mode-locked by nanotubes and graphene," *Physica E*, vol. 44, pp. 1082–1091, 2012.
[12] M. Chernysheva, A. Rozhin, Y. Fedotov, et al., "Carbon nanotubes for ultrafast fibre lasers," *Nanophotonics*, vol. 6, pp. 1–30, 2017.
[13] Q. Bao, H. Zhang, J. Yang, et al., "Graphene–polymer nanofiber membrane for ultrafast photonics," *Adv. Funct. Mater.*, vol. 20, pp. 782–791, 2010.
[14] R. I. Woodward, R. C. T. Howe, G. Hu, et al., "Few-layer MoS2 saturable absorbers for short-pulse laser technology: current status and future perspectives [Invited]," *Photonics Res.*, vol. 3, pp. A30–A42, 2015.
[15] H. Mu, S. Lin, Z. Wang, et al., "Black phosphorus–polymer composites for pulsed lasers," *Adv. Opt. Mater.*, vol. 3, pp. 1447–1453, 2015.
[16] Z.-C. Luo, M. Liu, H. Liu, et al., "2 GHz passively harmonic mode-locked fiber laser by a microfiber-based topological insulator saturable absorber," *Opt. Lett.*, vol. 38, pp. 5212–5215, 2013.
[17] P. Grelu and N. Akhmediev, "Dissipative solitons for mode-locked lasers," *Nat. Photonics*, vol. 6, pp. 84–92, 2012.
[18] K. Goda, D. R. Solli, K. K. Tsia and B. Jalali, "Theory of amplified dispersive Fourier transformation," *Phys. Rev. A*, vol. 80: 043821, 2009. https://doi.org/10.1103/physreva.80.043821.
[19] K. Goda, K. K. Tsia and B. Jalali, "Serial time-encoded amplified imaging for real-time observation of fast dynamic phenomena," *Nature*, vol. 458, pp. 1145–1149, 2009.
[20] K. Goda and B. Jalali, "Dispersive Fourier transformation for fast continuous single-shot measurements," *Nat. Photonics*, vol. 7, pp. 102–112, 2013.
[21] B. H. Kolner, "Space-time duality and the theory of temporal imaging," *IEEE J. Quantum Electron.*, vol. 30, pp. 1951–1963, 1994.
[22] C.-M. Tîlmaciu and M. C. Morris, "Carbon nanotube biosensors," *Front. Chem.*, vol. 3, pp. 1–21, 2015.
[23] S. Iijima, "Helical microtubules of graphitic carbon," *Nature*, vol. 354, pp. 56–58, 1991.
[24] D. S. Bethune, C. H. Kiang, M. S. De Vries, et al., "Cobalt-catalysed growth of carbon nanotubes with single-atomic-layer walls," *Nature*, vol. 363, pp. 605–657, 1993.
[25] S. Iijima and T. Ichihashi, "Single-shell carbon nanotubes of 1-nm diameter," *Nature*, vol. 363, pp. 603–605, 1993.
[26] T. W. Odom, J.-L. Huang, P. Kim and C. M. Lieber, "Atomic structure and electronic properties of single-walled carbon nanotubes," *Nature*, vol. 391, pp. 62–64, 1998.
[27] H. Kataura, Y. Kumazawa, Y. Maniwa, et al., "Optical properties of single-wall carbon nanotubes," *Synth. Met.*, vol. 103, pp. 2555–2558, 1999.
[28] T. Hasan, Z. Sun, F. Wang, et al., "Nanotube–polymer composites for ultrafast photonics," *Adv. Mater.*, vol. 21, pp. 3874–3899, 2009.
[29] G. Dresselhaus, M. S. Dresselhaus and S. Riichiro. *Physical Properties of Carbon Nanotubes*, MA, USA, World Scientific, 1998.
[30] M. Ouyang, J.-L. Huang, C. L. Cheung and C. M. Lieber, "Energy gaps in "Metallic" single-walled carbon nanotubes," *Science*, vol. 292, pp. 702–705, 2001.
[31] A. Martinez, K. Zhou, I. Bennion and S. Yamashita, "In-fiber microchannel device filled with a carbon nanotube dispersion for passive mode-lock lasing," *Opt. Express*, vol. 16, pp. 15425–15430, 2008.

[32] Y.-W. Song, S. Yamashita, C. S. Goh and S. Y. Set, "Carbon nanotube mode lockers with enhanced nonlinearity via evanescent field interaction in D-shaped fibers," *Opt. Lett.*, vol. 32, pp. 148–150, 2007.
[33] Y.-W. Song, K. Morimune, S. Y. Set and S. Yamashita, "Polarization insensitive all-fiber mode-lockers functioned by carbon nanotubes deposited onto tapered fibers," *Appl. Phys. Lett.*, vol. 90: 021101, 2007. https://doi.org/10.1063/1.2431445.
[34] S. Y. Choi, F. Rotermund, H. Jung, K. Oh and D. I. Yeom, "Femtosecond mode-locked fiber laser employing a hollow optical fiber filled with carbon nanotube dispersion as saturable absorber," *Opt. Express*, vol. 17, pp. 21788–21793, 2009.
[35] E. D. Obraztsova, A. V. Tausenev and A. I. Chernov, "Toward saturable absorbers for solid state lasers in form of holey fibers filled with single-wall carbon nanotubes," *Phys. Status Solidi*, vol. 247, pp. 3080–3083, 2010.
[36] X. Liu, D. Han, Z. Sun, et al., "Versatile multi-wavelength ultrafast fiber laser mode-locked by carbon nanotubes," *Sci. Rep.*, vol. 3, pp. 2718, 2013.
[37] F. Wang, A. G. Rozhin, V. Scardaci, et al., "Wideband-tuneable, nanotube mode-locked, fibre laser," *Nat. Nanotechnol.*, vol. 3, pp. 738–742, 2008.
[38] J. W. Nicholson, R. S. Windeler and D. J. DiGiovanni, "Optically driven deposition of single-walled carbon-nanotube saturable absorbers on optical fiber end-faces," *Opt. Express*, vol. 15, pp. 9176–9183, 2007.
[39] S. Yamashita, "A tutorial on nonlinear photonic applications of carbon nanotube and graphene," *J. Light Technol.*, vol. 30, pp. 427–447, 2012.
[40] A. Martinez, B. Xu and S. Yamashita, "Nanotube based nonlinear fiber devices for fiber lasers," *IEEE J. Sel. Top Quantum Electron.*, vol. 20, pp. 89–98, 2014.
[41] S. Yamashita, A. Martinez and B. Xu, "Short pulse fiber lasers mode-locked by carbon nanotubes and graphene," *Opt. Fiber Technol.*, vol. 20, pp. 702–713, 2014.
[42] B. Guo, Q. Xiao, S. Wang and H. Zhang, "2D layered materials, pp. synthesis, nonlinear optical properties, and device applications," *Laser Photon Rev.*, vol. 13, p. 1800327, 2019.
[43] S. Li, C. Wang, Y. Yin, E. Lewis and P. Wang, "Novel layered 2D materials for ultrafast photonics," *Nanophotonics*; 20200030, pp. 1–44, 2020.
[44] Y.-W. Song, S. Yamashita and S. Maruyama, "Single-walled carbon nanotubes for high-energy optical pulse formation," *Appl. Phys. Lett.*, vol. 92, pp. 21115, 2008.
[45] K. H. Fong, K. Kikuchi, C. S. Goh, et al., "Solid-state Er:Yb:glass laser mode-locked by using single-wall carbon nanotube thin film," *Opt. Lett.*, vol. 32, pp. 38–40, 2007.
[46] A. Schmidt, S. Rivier, G. Steinmeyer, et al., "Passive mode locking of Yb:KLuW using a single-walled carbon nanotube saturable absorber," *Opt. Lett.*, vol. 33, pp. 729–731, 2008.
[47] D. V. Khudyakov, A.S. Lobach and V. A. Nadtochenko, "Passive mode locking in a Ti:sapphire laser using a single-walled carbon nanotube saturable absorber at a wavelength of 810 nm," *Opt. Lett.*, vol. 35, pp. 2675–2677, 2010.
[48] H.-R. Chen, Y.-G. Wang, C.-Y. Tsai, et al., "High-power, passively mode-locked Nd:GdVO4laser using single-walled carbon nanotubes as saturable absorber," *Opt. Lett.*, vol. 36, pp. 1284–1286, 2011.
[49] I. H. Baek, S. Y. Choi, H. W. Lee, et al., "Single-walled carbon nanotube saturable absorber assisted high-power mode-locking of a Ti:sapphire laser," *Opt. Express*, vol. 19, pp. 7833–7838, 2011.
[50] Y.-W. Song, S. Yamashita, C. S. Goh and S. Y. Set, "Passively mode-locked lasers with 17.2-GHz fundamental-mode repetition rate pulsed by carbon nanotubes," *Opt. Lett.*, vol. 32, pp. 430–432, 2007.
[51] G. D. Valle, R. Osellame, G. Galzerano, et al., "Passive mode locking by carbon nanotubes in a femtosecond laser written waveguide laser," *Appl. Phys. Lett.*, vol. 89, pp. 231115, 2006.
[52] W. Li, C. Zhu, X. Rong, et al., "Bidirectional red-light passively Q-switched all-fiber ring lasers with carbon nanotube saturable absorber," *J. Light Technol.*, vol. 36, pp. 2694–2701, 2018.
[53] C. Wei, Y. Lyu, H. Shi, et al., "Mid-infrared Q-switched and mode-locked fiber lasers at 2.87 μm based on carbon nanotube," *IEEE J. Sel. Top Quantum Electron.*, vol. 25, pp. 1100206, 2019.
[54] S. Kivistö, T. Hakulinen, A. Kaskela, et al., "Carbon nanotube films for ultrafast broadband technology," *Opt. Express*, vol. 17, pp. 2358–2363, 2009.
[55] T. Hasan, Z. Sun, P. Tan, et al., "Double-wall carbon nanotubes for wide-band, ultrafast pulse generation," *ACS Nano*, vol. 8, pp. 4836–4847, 2014.
[56] A. Martinez and S. Yamashita, "Multi-gigahertz repetition rate passively modelocked fiber lasers using carbon nanotubes," *Opt. Express*, vol. 19, pp. 6155–6163, 2011.
[57] Q. Huang, C. Zou, T. Wang, M. A. Araimi, A. Rozhin, and C. Mou, "Observation of 550 MHz passively harmonic mode-locked pulses at L-band in an Er-doped fiber laser using carbon nanotubes film," *Chinese Phys. B*, vol. 27, pp. 094210, 2018. https://doi.org/10.1088/1674-1056/27/9/094210.
[58] Q. Huang, Z. Huang, M. A. Araimi, A Rozhi, and Mou C, "2.4 GHz L-band passively harmonic mode locked Er-doped fiber laser based on carbon nanotubes film," *IEEE Photonics Technol. Lett.*, vol. 32, pp. 121–124, 2020.
[59] X. Zhao, Z. Zheng, L. Liu, et al., "Switchable, dual-wavelength passively mode-locked ultrafast fiber laser based on a single-wall carbon nanotube modelocker and intracavity loss tuning," *Opt. Express*, vol. 19, pp. 1168–1173, 2011.
[60] Z. Zhang, Y. Cai, J. Wang, H. Wan, and L. Zhang, "Switchable dual-wavelength cylindrical vector beam generation from a passively mode-locked fiber laser based on carbon nanotubes," *IEEE J. Sel. Top Quantum Electron.* vol. 24, p. 1100906, 2018.
[61] X. Liu and Y. Cui, "Flexible pulse-controlled fiber laser," *Sci. Rep.*, vol. 5, p. 9399, 2015.
[62] X. Liu, Y. Cui, D. Han, X. Yao, and Z. Sun, "Distributed ultrafast fibre laser," *Sci. Rep.*, vol. 5, p. 9101, 2015.
[63] Y. Meng, Y. Li, Y. Xu, and F. Wang, "Carbon nanotube mode-locked thulium fiber laser with 200 nm tuning range," *Sci. Rep.*, vol. 7, p. 45109, 2017.
[64] D. Li, H. Jussila, Y. Wang, et al., "Wavelength and pulse duration tunable ultrafast fiber laser mode-locked with carbon nanotubes," *Sci. Rep.*, vol. 8, p. 2738, 2018.
[65] R. Dai, Y. Meng, Y. Li, J. Qin, S. Zhu, and F. Wang, "Nanotube mode-locked, wavelength and pulsewidth tunable thulium fiber laser," *Opt. Express*, vol. 27, pp. 3518–3527, 2019.
[66] M. Jung, J. Koo, Y. M. Chang, P. Debnath, Y. W. Song, and J. H. Lee, "An all fiberized, 1.89-μm Q-switched laser employing carbon nanotube evanescent field interaction," *Laser Phys. Lett.*, vol. 9, pp. 669–673, 2012.

[67] X. Li, Y. Wang, Y. Wang, et al., "Nonlinear absorption of SWNT film and its effects to the operation state of pulsed fiber laser," *Opt. Express*, vol. 22, pp. 17227–17235, 2014.
[68] X. Xu, J. Zhai, Y. Chen, et al., "Well-aligned single-walled carbon nanotubes for optical pulse generation and laser operation states manipulation," *Carbon*, vol. 95, pp. 84–90, 2015.
[69] M. Chernysheva, C. Mou, R. Arif, et al., "High power Q-switched thulium doped fibre laser using carbon nanotube polymer composite saturable absorber," *Sci. Rep.*, vol. 6, p. 24220, 2016.
[70] W. Li, T. Du, J. Lan, et al., "716nm deep-red passively Q-switched Pr:ZBLAN all-fiber laser using a carbon-nanotube saturable absorber," *Opt. Lett.*, vol. 42, pp. 671–674, 2017.
[71] Y. Lü, C. Wei, H. Zhang, Z. Kang, G. Qin, and Y. Liu, "Wideband tunable passively Q-switched fiber laser at 2.8 μm using a broadband carbon nanotube saturable absorber," *Photonics Res.*, vol. 7, pp. 14–18, 2019.
[72] J. Lee, J. Koo, Y. M. Chang, P. Debnath, Y.-W. Song, and J. H. Lee, "Experimental investigation on a Q-switched, mode-locked fiber laser based on the combination of active mode locking and passive Q switching," *J. Opt. Soc. Am. B.*, vol. 29, pp. 1479–1485, 2012.
[73] X. Liu, D. Popa, and N. Akhmediev, "Revealing the transition dynamics from Q switching to mode locking in a soliton laser," *Phys. Rev. Lett.*, vol. 123: 093901, 2019. https://doi.org/10.1103/physrevlett.123.093901.
[74] X. Liu, X. Yao, and Y. Cui, "Real-time observation of the buildup of soliton molecules," *Phys. Rev. Lett.*, vol. 121: 023905, 2018. https://doi.org/10.1103/physrevlett.121.023905.
[75] X. Liu and M. Pang, "Revealing the buildup dynamics of harmonic mode-locking states in ultrafast lasers," *Laser Photonics Rev.*, vol. 13, p. 1800333, 2019.
[76] M. Nakazawa, S. Nakahara, T. Hirooka, M. Yoshida, T. Kaino, and K. Komatsu, "Polymer saturable absorber materials in the 1.5 μm band using poly-methyl-methacrylate and polystyrene with single-wall carbon nanotubes and their application to a femtosecond laser," *Opt. Lett.*, vol. 31, pp. 915–917, 2006.
[77] Y. Wang, S. Alam, E. D. Obraztsova, A. S. Pozharov, S. Y. Set, and S. Yamashita, "Generation of stretched pulses and dissipative solitons at 2 μm from an all-fiber mode-locked laser using carbon nanotube saturable absorbers," *Opt. Lett.*, vol. 41, pp. 3864–3867, 2016.
[78] A. A. Krylov, S. G. Sazonkin, V. A. Lazarev, et al., "Ultra-short pulse generation in the hybridly mode-locked erbium-doped all-fiber ring laser with a distributed polarizer," *Laser Phys. Lett.*, vol. 12, p. 65001, 2015.
[79] K. Kieu and F. W. Wise, "All-fiber normal-dispersion femtosecond laser," *Opt. Express*, vol. 16, pp. 11453–11458, 2008.
[80] M. Chernysheva, A. Bednyakova, M. Al Araimi, et al., "Double-wall carbon nanotube hybrid mode-locker in Tm-doped fibre laser: a novel mechanism for robust bound-state solitons generation," *Sci. Rep.*, vol. 7, p. 44314, 2017.
[81] V. Tsatourian, S. V. Sergeyev, C. Mou, et al., "Polarisation dynamics of vector soliton molecules in mode locked fibre laser," *Sci. Rep.*, vol. 3, p. 3154, 2013.
[82] K. Jiang, S. Fu, P. Shum, and C. Lin, "A wavelength-switchable passively harmonically mode-locked fiber laser with low pumping threshold using single-walled carbon nanotubes," *IEEE Photonics Technol. Lett.*, vol. 22, pp. 754–756, 2010.
[83] C. Mou, S. Sergeyev, A. Rozhin, and S. Turitsyn, "Vector solitons with slowly precessing states of polarization," *Opt. Express*, vol. 20, p. 3059–3061, 2012.
[84] C. Mou, S. Sergeyev, A. Rozhin, and S. Turistyn, "All-fiber polarization locked vector soliton laser using carbon nanotubes," *Opt. Lett.*, vol. 36, pp. 3831–3833, 2011.
[85] H. H. Liu and K. K. Chow, "Dark pulse generation in fiber lasers incorporating carbon nanotubes," *Opt. Express*, vol. 22, pp. 29708–29713, 2014.
[86] B. Fu, D. Popa, Z. Zhao, et al., "Wavelength tunable soliton rains in a nanotube-mode locked Tm-doped fiber laser," *Appl. Phys. Lett.*, vol. 113, p. 193102, 2018.
[87] H. J. Kbashi, S. V. Sergeyev, M. Al. Araimi, N. Tarasov, and A. Rozhin, "Vector soliton rain," *Laser Phys. Lett.*, vol. 16, p. 35103, 2019.
[88] Y. Zhang, D. Lu, H. Yu, and H. Zhang, "Low-dimensional saturable absorbers in the visible spectral region," *Adv. Opt. Mater.*, vol. 7, p. 1800886, 2019.
[89] F. Kaertner, L. Brovelli, D. Kopf, M. Kamp, I. Calasso, and U. Keller, "Control of solid state laser dynamics by semiconductor devices," *Opt. Eng.*, vol. 34, pp. 2024-2037, 1995.
[90] C. Hönninger, R. Paschotta, F. Morier-Genoud, M. Moser, and U. Keller, "Q-switching stability limits of continuous-wave passive mode locking," *J. Opt. Soc. Am. B.*, vol. 16, pp. 46–56, 1999.
[91] S. Y. Set, H. Yaguchi, Y. Tanaka, et al., "A dual-regime mode-locked/Q-switched laser using a saturable absorber incorporating carbon nanotubes (SAINT)," in *Conference on Lasers and Electro-Optics*, Baltimore, MD, USA, CLEO '03., 2003, pp. 3, 2003.
[92] X. Xu, S. Ruan, J. Zhai, L. Li, J. Pei, and Z. Tang, "Facile active control of a pulsed erbium-doped fiber laser using modulation depth tunable carbon nanotubes," *Photonics Res.*, vol. 6, pp. 996–1002, 2018.
[93] H. F. Ma, Y. G. Wang, W. Zhou, J. Y. Long, D. Y. Shen, and Y. S. Wang, "A passively Q-switched thulium-doped fiber laser with single-walled carbon nanotubes," *Laser Phys.*, vol. 23, p. 35109, 2013.
[94] N. Kasim, A. H. H. Al-Masoodi, F. Ahmad, Y. Munajat, H. Ahmad, and S. W. Harun, "Q-switched ytterbium doped fiber laser using multi-walled carbon nanotubes saturable absorber," *Chinese Opt. Lett.*, vol. 12, p. 31403, 2014.
[95] M. H. M. Ahmed, N. M. Ali, Z. S. Salleh, et al., "Q-switched erbium doped fiber laser based on single and multiple walled carbon nanotubes embedded in polyethylene oxide film as saturable absorber," *Opt. Laser Technol.*, vol. 65, pp. 25–28, 2015.
[96] B. Dong, J. Hao, J. Hu, and C. Liaw, "Wide pulse-repetition-rate range tunable nanotube Q-switched low threshold erbium-doped fiber laser," *IEEE Photonics Technol. Lett.*, vol. 22, pp. 1853–1855, 2010.
[97] A. Y. Chamorovskiy, A. V. Marakulin, A. S. Kurkov, T. Leinonen, and O. G. Okhotnikov, "High-repetition-rate Q-switched holmium fiber laser," *IEEE Photonics J.*, vol. 4, pp. 679–683, 2012.
[98] H. Ahmad, M. F. Ismail, and S. N. Aidit, "Optically modulated tunable O-band praseodymium-doped fluoride fiber laser utilizing multi-walled carbon nanotube saturable absorber," *Chinese Phys. Lett.*, vol. 36, p. 104202, 2019.
[99] B. Dong, J. Hu, C.-Y. Liaw, J. Hao, and C. Yu, "Wideband-tunable nanotube Q-switched low threshold erbium doped fiber laser," *Appl. Opt.*, vol. 50, pp. 1442–1445, 2011.

[100] Z. Yu, Y. Song, C. Tian, J. Li, X. Zhang, and Y. Wang, "Q-switched Yb-doped double cladding fiber laser with single wall carbon nanotube saturable absorber," In: High-Power Lasers and Applications VI International Society for Optics and Photonics, vol. 8551, p. 855115, 2012.
[101] A. H. H. Al-Masoodi, M. F. Ismail, F. Ahmad, et al., "Q-switched Yb-doped fiber laser operating at 1073 nm using a carbon nanotubes saturable absorber," *Microw. Opt. Technol. Lett.*, vol. 56, pp. 1770–1773, 2014.
[102] M. Z. Ab Razak, Z. Saleh, F. Ahmad, C. Anyi, S. Harun, and H. bin Arof, "High-power Q-switched erbium-ytterbium codoped fiber laser using multiwalled carbon nanotubes saturable absorber," *Opt. Eng.*, vol. 55, p. 106112, 2016.
[103] S. J. Tan, S. W. Harun, F. Ahmad, R. M. Nor, N. R. Zulkepely, and H. Ahmad, "A Q-switched multi-wavelength Brillouin erbium fiber laser with a single-walled carbon nanotube saturable absorber," *Laser. Phys.*, vol. 23, p. 55101, 2013.
[104] Z. C. Tiu, F. Ahmad, S. J. Tan, A. Zarei, H. Ahmad, and S. W. Harun, "Multi-wavelength Q-switched Erbium-doped fiber laser with photonic crystal fiber and multi-walled carbon nanotubes," *J. Mod. Opt.*, vol. 61, pp. 1133–1139, 2014.
[105] H. Ahmad, S. N. M. Hassan, F. Ahmad, M. Z. Zulkifli, and S. W. Harun, "Broadband tuning in a passively Q-switched erbium doped fiber laser (EDFL) via multiwall carbon nanotubes/ polyvinyl alcohol (MWCNT/PVA) saturable absorber," *Opt. Commun.*, vol. 365, pp. 54–60, 2016.
[106] M. Z. Zulkifli, F. D. Muhammad, M. F. Mohd Azri, et al., "Tunable passively Q-switched ultranarrow linewidth erbium-doped fiber laser," *Results Phys.*, vol. 16, p. 102949, 2020.
[107] B. Dong, C. -Y. Liaw, J. Hao, and J. Hu, "Nanotube Q-switched low-threshold linear cavity tunable erbium-doped fiber laser," *Appl. Opt.*, vol. 49, pp. 5989–5992, 2010.
[108] D. Zhou, L. Wei, B. Dong, and W. Liu, "Tunable passively Q-switched erbium-doped fiber laser with carbon nanotubes as a saturable absorber," *IEEE Photonics Technol. Lett.*, vol. 22, pp. 9–11, 2010.
[109] B. Dong, J. Hu, C. Yu, and J. Hao, "Multi-wavelength Q-switched erbium doped fiber laser with a short carbon nanotube based saturable absorber," *Opt. Commun.*, vol. 285, pp. 3864–3867, 2012.
[110] L. Liu, Z. Zheng, X. Zhao, et al., "Dual-wavelength passively Q-switched Erbium doped fiber laser based on an SWNT saturable absorber," *Opt. Commun.*, vol. 294, pp. 267–270, 2013.
[111] H. Ahmad, A. Muhamad, A. S. Sharbirin, M. Z. Samion, and M. F. Ismail, "Tunable Q-switched thulium-doped Fiber Laser using multiwall carbon nanotube and Fabry-Perot Etalon filter," *Opt. Commun.*, vol. 383, pp. 359–365, 2017.
[112] N. Saidin, D. I. M. Zen, F. Ahmad, et al., "Q-switched 2μm thulium bismuth co-doped fiber laser with multi-walled carbon nanotubes saturable absorber," *Opt. Laser Technol.*, vol. 83, pp. 89–93, 2016.
[113] F. Wang, Z. Jiang, T. Hasan, et al., "Double-wall carbon nanotube Q-switched and mode-locked two-micron fiber lasers," in *Conference on Lasers and Electro-Optics 2012 (Optical Society of America)*, p. CF1N.4, 2012.
[114] S. Xu, F. Wang, C. Zhu, et al., "Ultrafast nonlinear photoresponse of single-wall carbon nanotubes: a broadband degenerate investigation," *Nanoscale*, vol. 8, pp. 9304–9309, 2016.
[115] G. P. Agrawal. *Nonlinear Fiber Optics*. NY, USA, Academic Press, 2007.
[116] S. Set, H. Yaguchi, M. Jablonski, et al., "A noise suppressing saturable absorber at 1550nm based on carbon nanotube technology," in *Optical Fiber Communication Conference 2003*, Atlanta, GA, USA, vol. p. FL2, 2003.
[117] S. Y. Set, H. Yaguchi, Y. Tanaka, and M. Jablonski, "Laser mode locking using a saturable absorber incorporating carbon nanotubes," *J. Light Technol.*, vol. 22, p. 51, 2004.
[118] A. G. Rozhin, Y. Sakakibara, S. Namiki, M. Tokumoto, H. Kataura, and Y. Achiba, "Sub-200-fs pulsed erbium-doped fiber laser using a carbon nanotube-polyvinylalcohol mode locker," *Appl. Phys. Lett.*, vol. 88, p. 51118, 2006.
[119] F. Shohda, T. Shirato, M. Nakazawa, K. Komatsu, and T. Kaino, "A passively mode-locked femtosecond soliton fiber laser at 1.5 μm with a CNT-doped polycarbonate saturable absorber," *Opt. Express*, vol. 16, pp. 21191–21198, 2008.
[120] M. A. Ismail, S. W. Harun, N. R. Zulkepely, R. M. Nor, F. Ahmad, and H. Ahmad, "Nanosecond soliton pulse generation by mode-locked erbium-doped fiber laser using single-walled carbon-nanotube-based saturable absorber," *Appl. Opt.*, vol. 51, pp. 8621–8624, 2012.
[121] R. I. Woodward, E. J. R. Kelleher, D. Popa, et al., "Scalar nanosecond pulse generation in a nanotube mode-locked environmentally stable fiber laser," *IEEE Photonics Technol. Lett.*, vol. 26, pp. 1672–1675, 2014.
[122] C. Mou, A. G. Rozhin, R. Arif, K. Zhou, and S. Turitsyn, "Polarization insensitive in-fiber mode-locker based on carbon nanotube with N-methyl-2-pryrrolidone solvent filled fiber microchamber," *Appl. Phys. Lett.*, vol. 100, p. 101110, 2012.
[123] X. K. Yao, "Three types of pulses delivered from a nanotube-mode-locked fiber laser," *Laser Phys.*, vol. 25: 075101, 2015. https://doi.org/10.1088/1054-660x/25/7/075101.
[124] E. J. R. Kelleher, J. C. Travers, Z. Sun, et al., "Bismuth fiber integrated laser mode-locked by carbon nanotubes," *Laser Phys. Lett.*, vol. 7, pp. 790–794, 2010.
[125] S. Yong-Won, S. Y. Set, S. Yamashita, C. S. Goh, and T. Kotake, "1300-nm pulsed fiber lasers mode-locked by purified carbon nanotubes," *IEEE Photonics Technol. Lett.*, vol. 17, pp. 1623–1625, 2005.
[126] G. Sobon, A. Duzynska, M. Świniarski, J. Judek, J. Sotor, and M. Zdrojek, "CNT-based saturable absorbers with scalable modulation depth for Thulium-doped fiber lasers operating at 1.9 μm," *Sci. Rep.*, vol. 7, pp. 1–9, 2017.
[127] M. Pawliszewska, A. Dużyńska, M. Zdrojek, and J. Sotor, "Metallic carbon nanotube-based saturable absorbers for holmium-doped fiber lasers," *Opt. Express*, vol. 27, pp. 11361–11369, 2019.
[128] C. S. Goh, K. Kikuchi, S. Y. Set, et al., "Femtosecond mode-locking of a ytterbium-doped fiber laser using a carbon-nanotube-based mode-locker with ultra-wide absorption band," In *Conference on Lasers and Electro-Optics, 2005*, Baltimore, MD, 3, pp. 1644–1646, 2005.
[129] N. Nishizawa, Y. Seno, K. Sumimura, et al., "All-polarization-maintaining Er-doped ultrashort-pulse fiber laser using carbon nanotube saturable absorber," *Opt. Express*, vol. 16, pp. 9429–9435, 2008.
[130] F. Shohda, T. Shirato, M. Nakazawa, J. Mata, and J. Tsukamoto, "147 fs, 51 MHz soliton fiber laser at 1.56 μm with a fiber-

connector-type SWNT/P3HT saturable absorber," *Opt. Express*, vol. 16, pp. 20943–20948, 2008.
[131] M. A. Chernysheva, A. A. Krylov, P. G. Kryukov, et al., "Thulium-doped mode-locked all-fiber laser based on NALM and carbon nanotube saturable absorber," *Opt. Express*, vol. 20, pp. B124–B130, 2012.
[132] M. A. Solodyankin, E. D. Obraztsova, A. S. Lobach, et al., "Mode-locked 1.93 μm thulium fiber laser with a carbon nanotube absorber," *Opt. Lett.*, vol. 33, pp. 1336–1338, 2008.
[133] A. Y. Chamorovskiy, A. V. Marakulin, A. S. Kurkov, and O. G. Okhotnikov, "Tunable Ho-doped soliton fiber laser mode-locked by carbon nanotube saturable absorber," *Laser Phys. Lett.*, vol. 9, pp. 602–606, 2012.
[134] C. Wei, Y. Lyu, Q. Li, et al., "Wideband tunable, carbon nanotube mode-locked fiber laser emitting at wavelengths around 3 μm," *IEEE Photonics Technol. Lett.*, vol. 31, pp. 869–872, 2019.
[135] D. Popa, Z. Sun, T. Hasan, et al., "74-fs nanotube-mode-locked fiber laser," *Appl. Phys. Lett.*, vol. 101, p. 153107, 2012.
[136] Z. Yu, Y. Wang, X. Zhang, X. Dong, J. Tian, and Y. Song, "A 66 fs highly stable single wall carbon nanotube mode locked fiber laser," *Laser. Phys.*, vol. 24, p. 15105, 2013.
[137] Y. Chen, F. X. Kärtner, U. Morgner, et al., "Dispersion-managed mode locking," *J. Opt. Soc. Am. B.*, vol. 16, pp. 1999–2004, 1999.
[138] H. A. Haus, K. Tamura, L. E. Nelson, and E. P. Ippen, "Stretched-pulse additive pulse mode-locking in fiber ring lasers: theory and experiment," *IEEE J. Quantum Electron.*, vol. 31, pp. 591–598, 1995.
[139] W. S. Kwon, H. Lee, J. H. Kim, J. Choi, K. -S. Kim, and S. Kim, "Ultrashort stretched-pulse L-band laser using carbon-nanotube saturable absorber," *Opt. Express*, vol. 23, pp. 7779–7785, 2015.
[140] J. Wang, Z. Cai, P. Xu, et al., "Pulse dynamics in carbon nanotube mode-locked fiber lasers near zero cavity dispersion," *Opt. Express*, vol. 23, pp. 9947–9958, 2015.
[141] X. Han, "Conventional soliton or stretched pulse delivered by nanotube-mode-locked fiber laser," *Appl. Opt.* , vol. 57, pp. 807–811, 2018.
[142] L. Hou, H. Guo, Y. Wang, et al., "Sub-200 femtosecond dispersion-managed soliton ytterbium-doped fiber laser based on carbon nanotubes saturable absorber," *Opt. Express*, vol. 26, pp. 9063–9070, 2018.
[143] K. Watanabe, Y. Zhou, A. Saitoh, Y. Sakakibara, and N. Nishizawa, "Dispersion Managed, High Power Tm-doped Ultrashort Pulse Fiber Laser at 1.9 um Using Single Wall Carbon Nanotube Polyimide Film," in *Conference on Lasers and Electro-Optics (Optical Society of America)*, p. JW2A.98, 2019.
[144] Z. Sun, A. G. Rozhin, F. Wang, et al., "Ultrafast erbium-doped fiber laser mode-locked by a carbon nanotube saturable absorber," in *Conference on Lasers and Electro-Optics/ International Quantum Electronics Conference (Optical Society of America)*, p. CML5, 2009.
[145] F. Shohda, M. Nakazawa, J. Mata, and J. Tsukamoto, "A 113 fs fiber laser operating at 1.56 μm using a cascadable film-type saturable absorber with P3HT-incorporated single-wall carbon nanotubes coated on polyamide," *Opt. Express*, vol. 18, pp. 9712–9721, 2010.
[146] Z. Sun, T. Hasan, F. Wang, A. G. Rozhin, I. H. White, and A. C. Ferrari, "Ultrafast stretched-pulse fiber laser mode-locked by carbon nanotubes," *Nano Res.*, vol. 3, pp. 404–411, 2010.
[147] A. Martinez and S. Yamashita, "Stretch-pulse mode-locking employing a carbon nanotube saturable absorber," in *17th Microopics Conference (MOC)*, Sendai, pp. 1–2, 2011.
[148] N. Nishizawa, Y. Nozaki, E. Itoga, H. Kataura, Y. Sakakibara, "Dispersion-managed, high-power, Er-doped ultrashort-pulse fiber laser using carbon-nanotube polyimide film," *Opt. Express*, vol. 19, pp. 21874–21879, 2011.
[149] X. Yao, "Generation of bidirectional stretched pulses in a nanotube-mode-locked fiber laser," *Appl. Opt.*, vol. 53, pp. 27–31, 2014.
[150] V. Lazarev, A. Krylov, D. Dvoretskiy, et al., "Stable similariton generation in an all-fiber hybrid mode-locked ring laser for frequency metrology," *IEEE. Trans. Ultrason. Ferroelectr. Freq. Control.*, vol. 63, pp. 1028–1033, 2016.
[151] H. Jeong, S. Y. Choi, F. Rotermund, Y.-H. Cha, D.-Y. Jeong, and D.-I. Yeom, "All-fiber mode-locked laser oscillator with pulse energy of 34 nJ using a single-walled carbon nanotube saturable absorber," *Opt. Express*, vol. 22, pp. 22667–22672, 2014.
[152] B. Oktem, C. Ülgüdür, and F. Ö. Ilday, "Soliton–similariton fibre laser," *Nat. Photonics*, vol. 4, pp. 307–311, 2010.
[153] K. Kieu and F. W. Wise, "Self-similar and stretched-pulse operation of erbium-doped fiber lasers with carbon nanotubes saturable absorber," in *Conference on Lasers and Electro-Optics/International Quantum Electronics Conference (Optical Society of America)*, p. CML3, 2009.
[154] X. Li, Y. Wang, Y. Wang, et al., "Wavelength-switchable and wavelength-tunable all-normal-dispersion mode-locked Yb-doped fiber laser based on single-walled carbon nanotube wall paper absorber," *IEEE Photonics J.*, vol. 4, pp. 234–241, 2012.
[155] Y. Cui and X. Liu, "Graphene and nanotube mode-locked fiber laser emitting dissipative and conventional solitons," *Opt. Express*, vol. 21, pp. 18969–18974, 2013.
[156] Y. D. Cui, X. M. Liu, and C. Zeng, "Conventional and dissipative solitons in a CFBG-based fiber laser mode-locked with a graphene–nanotube mixture," *Laser Phys. Lett.*, vol. 11, p. 55106, 2014.
[157] J. H. Im, S. Y. Choi, F. Rotermund, and D. -I. Yeom, "All-fiber Er-doped dissipative soliton laser based on evanescent field interaction with carbon nanotube saturable absorber," *Opt. Express*, vol. 18, pp. 22141–22146, 2010.
[158] Z. Sun, A. G. Rozhin, F. Wang, et al., "A compact, high power, ultrafast laser mode-locked by carbon nanotubes," *Appl. Phys. Lett.*, vol. 95, p. 253102, 2009.
[159] B. Xu, A. Martinez, S. Y. Set, C. S. Goh, and S. Yamashita, "A net normal dispersion all-fiber laser using a hybrid mode-locking mechanism," *Laser Phys. Lett.*, vol. 11, p. 25101, 2013.
[160] A. Khegai, M. Melkumov, S. Firstov, et al., "Bismuth-doped fiber laser at 1.32 μm mode-locked by single-walled carbon nanotubes," *Opt. Express*, vol. 26, pp. 23911–23917, 2018.
[161] Q. Wang, T. Chen, M. Li, B. Zhang, Y. Lu, and K. P. Chen, "All-fiber ultrafast thulium-doped fiber ring laser with dissipative soliton and noise-like output in normal dispersion by single-wall carbon nanotubes. *Appl. Phys. Lett.*, vol. 103, p. 11103, 2013.
[162] C. E. S. Castellani, E. J. R. Kelleher, D. Popa, et al., "CW-pumped short pulsed 1.12 μm Raman laser using carbon nanotubes," *Laser Phys. Lett.*, vol. 10, p. 15101, 2012.
[163] C. E. S. Castellani, E. J. R. Kelleher, J. C. Travers, et al., "Ultrafast Raman laser mode-locked by nanotubes," *Opt. Lett.*, vol. 36, pp. 3996–3998, 2011.

[164] Y. Z. Pan, J. G. Miao, W. J. Liu, X. J. Huang, and Y. B. Wang, "Mode-locked ytterbium fiber lasers using a large modulation depth carbon nanotube saturable absorber without an additional spectral filter," *Laser Phys. Lett.*, vol. 11, p. 95105, 2014.
[165] M. E. Fermann and I. Hartl, "Ultrafast fibre lasers," *Nat. Photonics*, vol. 7, pp. 868–74, 2013.
[166] T. Udem, R. Holzwarth, and T. W. Hänsch, "Optical frequency metrology," *Nature*, vol. 416, pp. 233–237, 2002.
[167] C. Kerse, H. Kalaycıoğlu, P. Elahi, et al., "Ablation-cooled material removal with ultrafast bursts of pulses," *Nature*, vol. 537, pp. 84–88, 2016.
[168] C. Mou, R. Arif, A. Rozhin, and S. Turitsyn, "Passively harmonic mode locked erbium doped fiber soliton laser with carbon nanotubes based saturable absorber," *Opt. Mater. Express*, vol. 2, pp. 884–890, 2012.
[169] A. A. Mkrtchyan, Y. G. Gladush, D. Galiakhmetova, V. Yakovlev, V. T. Ahtyamov, and A. G. Nasibulin, "Dry-transfer technique for polymer-free single-walled carbon nanotube saturable absorber on a side polished fiber," *Opt. Mater. Express*, vol. 9, pp. 1551–1561, 2019.
[170] S. Yamashita, T. Yoshida, S. Set, P. Polynkin, and N. Peyghambarian, "Passively mode-locked short-cavity 10GHz Er:Yb-codoped phosphate-fiber laser using carbon nanotubes," in: *Fiber Lasers IV: Technology, Systems, and Applications*, International Society for Optics and Photonics, vol. 6453, p. 64531Y, 2007.
[171] Y. Senoo, N. Nishizawa, Y. Sakakibara, et al., "Polarization-maintaining, high-energy, wavelength-tunable, Er-doped ultrashort pulse fiber laser using carbon-nanotube polyimide film," *Opt. Express*, vol. 17, pp. 20233–20241, 2009.
[172] R. Going, D. Popa, F. Torrisi, et al., "500fs wideband tunable fiber laser mode-locked by nanotubes," *Physica E*, vol. 44, pp. 1078–1081, 2012.
[173] C. Zou, T. Wang, Z. Yan, et al., "Wavelength-tunable passively mode-locked Erbium-doped fiber laser based on carbon nanotube and a 45° tilted fiber grating," *Opt. Commun.*, vol. 406, pp. 151–157, 2018.
[174] Y. Liu, X. Zhao, J. Liu, G. Hu, Z. Gong, and Z. Zheng, "Widely-pulsewidth-tunable ultrashort pulse generation from a birefringent carbon nanotube mode-locked fiber laser," *Opt. Express*, vol. 22, pp. 21012–21017, 2014.
[175] F. Wang, Z. Jiang, Z. Sun, et al., "Dual-wavelength, carbon nanotube mode-locked fiber laser," in *IEEE Photonics Conference 2012*, pp. 505–506, 2012.
[176] R. Wang, X. Zhao, W. Bai, J. Chen, Y. Pan, and Z. Zheng, "Polarization-maintaining, dual-wavelength, dual-comb mode-locked fiber laser," n: *Conference on Lasers and Electro-Optics (Optical Society of America)*, p. JTh2A.139, 2018.
[177] L. Gui, P. Wang, Y. Ding, et al., "Soliton molecules and multisoliton states in ultrafast fibre lasers: intrinsic complexes in dissipative systems," *Appl. Sci.*, vol. 8, p. 201, 2018.
[178] M. Liu, A. -P. Luo, Y. -R. Yan, et al., "Successive soliton explosions in an ultrafast fiber laser," *Opt. Lett.*, vol. 41, pp. 1181–1184, 2016.
[179] M. Liu, A. -P. Luo, W. -C. Xu, and Z. -C. Luo, "Dissipative rogue waves induced by soliton explosions in an ultrafast fiber laser," *Opt. Lett.*, vol. 41, pp. 3912–3915, 2016.
[180] H. -J. Chen, Y. -J. Tan, J. -G. Long, et al., "Dynamical diversity of pulsating solitons in a fiber laser," *Opt. Express*, vol. 27, pp. 28507–28522, 2019.
[181] M. Liu, A. -P. Luo, Z. -C. Luo, and W. -C. Xu, "Dynamic trapping of a polarization rotation vector soliton in a fiber laser," *Opt. Lett.*, vol. 42, pp. 330–333, 2017.
[182] H. Zhang, D. Y. Tang, L. M. Zhao, and X. Wu, "Dark pulse emission of a fiber laser," *Phys. Rev. A.*, vol. 80: 045803, 2009. https://doi.org/10.1103/physreva.80.045803.
[183] J. B. Schroeder, S. Coen, T. Sylvestre, and B. J. Eggleton, "Dark and bright pulse passive mode-locked laser with in-cavity pulse-shaper," *Opt. Express*, vol. 18, pp. 22715–22721, 2010.
[184] D. Y. Tang, L. Li, Y. F. Song, L. M. Zhao, H. Zhang, and D. Y. Shen, "Evidence of dark solitons in all-normal-dispersion-fiber lasers," *Phys. Rev. A.*, vol. 88: 013849, 2013. https://doi.org/10.1103/physreva.88.013849.
[185] H. Zhang, D. Tang, L. Zhao, and X. Wu, "Dual-wavelength domain wall solitons in a fiber ring laser," *Opt. Express*, vol. 19, pp. 3525–3530, 2011.
[186] H. H. Liu and K. K. Chow, "Dark pulse generation in fiber lasers incorporating carbon nanotubes," *Opt. Express*, vol. 22, pp. 29708–29713, 2014.
[187] S. Chouli and P. Grelu, "Rains of solitons in a fiber laser," *Opt. Express*, vol. 17, pp. 11776–11781, 2009.
[188] S. Chouli and P. Grelu, "Soliton rains in a fiber laser: an experimental study," *Phys. Rev. A.*, vol. 81: 063829, 2010. https://doi.org/10.1103/physreva.81.063829.
[189] C. Bao, X. Xiao, and C. Yang, "Soliton rains in a normal dispersion fiber laser with dual-filter," *Opt. Lett.*, vol. 38, pp. 1875–1877, 2013.
[190] K. Sulimany, O. Lib, G. Masri, et al., "Bidirectional soliton rain dynamics induced by casimir-like interactions in a graphene mode-locked fiber laser," *Phys. Rev. Lett.*, vol. 121, p. 133902, 2018.
[191] H. Kbashi, S. V. Sergeyev, C. Mou, et al., "Bright-dark rogue waves," *Ann. Phys.*, vol. 530: 1700362, 2018.
[192] A. Hasegawa and F. Tappert, "Transmission of stationary nonlinear optical pulses in dispersive dielectric fibers. I. Anomalous dispersion," *Appl. Phys. Lett.*, vol. 23, pp. 142–144, 1973.
[193] L. F. Mollenauer, R. H. Stolen, and J. P. Gordon, "Experimental observation of picosecond pulse narrowing and solitons in optical fibers," *Phys. Rev. Lett.*, vol. 45, pp. 1095–1098, 1980.
[194] L. E. Nelson, D. J. Jones, K. Tamura, H. A. Haus, and E. P. Ippen, "Ultrashort-pulse fiber ring lasers," *Appl. Phys. B.*, vol. 65, pp. 277–294, 1997.
[195] C. Lecaplain, P. Grelu, J. M. Soto-Crespo, and N. Akhmediev, "Dissipative rogue waves generated by chaotic pulse bunching in a mode-locked laser," *Phys. Rev. Lett.*, vol. 108, p. 233901, 2012.
[196] E. G. Turitsyna, S. V. Smirnov, S. Sugavanam, et al., "The laminar-turbulent transition in a fibre laser," *Nat. Photonics*, vol. 7, pp. 783–786, 2013.
[197] W. Chang, A. Ankiewicz, J. M. Soto-Crespo, and N. Akhmediev, "Dissipative soliton resonances," *Phys. Rev. A*, vol. 78: 023830, 2008. https://doi.org/10.1103/physreva.78.023830.
[198] D. Mao, X. M. Liu, L. R. Wang, X. H. Hu, and H. Lu, "Partially polarized wave-breaking-free dissipative soliton with super-broad spectrum in a mode-locked fiber laser," *Laser Phys. Lett.*, vol. 8, pp. 134–138, 2011.
[199] L. Duan, X. Liu, D. Mao, L. Wang, and G. Wang, "Experimental observation of dissipative soliton resonance in an anomalous-

dispersion fiber laser," *Opt. Express*, vol. 20, pp. 265–270, 2012.
[200] X. Liu, "Pulse evolution without wave breaking in a strongly dissipative-dispersive laser system," *Phys. Rev. A*, vol. 81: 053819, 2010. https://doi.org/10.1103/physreva.81.053819.
[201] X. Liu, "Mechanism of high-energy pulse generation without wave breaking in mode-locked fiber lasers," *Phys. Rev. A*, vol. 82: 053808, 2010. https://doi.org/10.1103/physreva.82.053808.
[202] D. Y. Tang, W. S. Man, H. Y. Tam, and P. D. Drummond, "Observation of bound states of solitons in a passively mode-locked fiber laser," *Phys. Rev. A*, vol. 64: 033814, 2001. https://doi.org/10.1103/physreva.64.033814.
[203] X. Li, X. Liu, X. Hu, et al., "Long-cavity passively mode-locked fiber ring laser with high-energy rectangular-shape pulses in anomalous dispersion regime," *Opt. Lett.*, vol. 35, pp. 3249–3251, 2010.
[204] X. Liu, "Numerical and experimental investigation of dissipative solitons in passively mode-locked fiber lasers with large net-normal-dispersion and high nonlinearity," *Opt. Express*, vol. 17, pp. 22401–22416, 2009.
[205] K. Goda, K. K. Tsia, and B. Jalali, "Amplified dispersive Fourier-transform imaging for ultrafast displacement sensing and barcode reading," *Appl. Phys. Lett.*, vol. 93, p. 131109, 2008.
[206] K. Goda, A. Ayazi, D. R. Gossett, et al., "High-throughput single-microparticle imaging flow analyzer," *Proc. Natl. Acad. Sci. U S A*, vol. 109, p. 11630–11635, 2012.
[207] X. Wei, A. K. S. Lau, Y. Xu, et al., "Broadband fiber-optical parametric amplification for ultrafast time-stretch imaging at 1.0 μm," *Opt. Lett.*, vol. 39, pp. 5989–5992, 2014.
[208] L. Golan, D. Yeheskely-Hayon, L. Minai, E. J. Dann, and D. Yelin, "Noninvasive imaging of flowing blood cells using label-free spectrally encoded flow cytometry," *Biomed. Opt. Express*, vol. 3, pp. 1455–1464, 2012.
[209] Y. Jiang, S. Karpf, and B. Jalali, "Time-stretch LiDAR as a spectrally scanned time-of-flight ranging camera," *Nat. Photonics*, vol. 14, pp. 14–18, 2020.
[210] D. R. Solli, J. Chou, and B. Jalali, "Amplified wavelength-time transformation for real-time spectroscopy," *Nat. Photonics*, vol. 2, pp. 48–51, 2008.
[211] B. Jalali and A. Mahjoubfar, "Tailoring wideband signals with a photonic hardware accelerator," *Proc. IEEE*, vol. 103, pp. 1071–1086, 2015.
[212] B. Jalali and S. Yegnanarayanan, "Optically controlled phased-array antenna using wavelength-selective true time delay," *IEEE Int. Symp. Phased Array Syst. Technol.*, vol. 367–370, 2000.
[213] E. D. Diebold, N. K. Hon, Z. Tan, et al., "Giant tunable optical dispersion using chromo-modal excitation of a multimode waveguide," *Opt. Express*, vol. 19, pp. 23809–23817, 2011.
[214] S. Yegnanarayanan, P. D. Trinh, and B. Jalali, "Recirculating photonic filter: a wavelength-selective time delay for phased-array antennas and wavelength code-division multiple access," *Opt. Lett.*, vol. 21, pp. 740–742, 1996.
[215] S. Hamdi, A. Coillet, and P. Grelu, "Real-time characterization of optical soliton molecule dynamics in an ultrafast thulium fiber laser," *Opt. Lett.*, vol. 43, pp. 4965–4968, 2018.
[216] X. Liu and Y. Cui, "Revealing the behavior of soliton buildup in a mode-locked laser," *Adv. Photonics*, vol. 1: 016003, 2019. https://doi.org/10.1117/1.ap.1.1.016003.
[217] P. Ryczkowski, M. Närhi, C. Billet, J. -M. Merolla, G. Genty, and J. M. Dudley, "Real-time full-field characterization of transient dissipative soliton dynamics in a mode-locked laser," *Nat. Photonics*, vol. 12, pp. 221–227, 2018.
[218] J. Peng, M. Sorokina, S. Sugavanam, et al., "Real-time observation of dissipative soliton formation in nonlinear polarization rotation mode-locked fibre lasers," *Commun. Phys.*, vol. 1, pp. 1–8, 2018.
[219] G. Herink, B. Jalali, C. Ropers, and D. R. Solli, "Resolving the build-up of femtosecond mode-locking with single-shot spectroscopy at 90 MHz frame rate," *Nat. Photonics*, vol. 10, pp. 321–326, 2016.
[220] D. Abraham, R. Nagar, V. Mikhelashvili, and G. Eisenstein, "Transient dynamics in a self-starting passively mode-locked fiber-based soliton laser," *Appl. Phys. Lett.*, vol. 63, pp. 2857–2859, 1993.
[221] J. -C. Kuo and C. -L. Pan, "Buildup of steady-state subpicosecond and femtosecond pulses in a colliding-pulse mode-locked ring dye laser," *Opt. Lett.*, vol. 15, pp. 1297–1299, 1990.
[222] F. Krausz, T. Brabec, and C. Spielmann, "Self-starting passive mode locking," *Opt. Lett.*, vol. 16, pp. 235–237, 1991.
[223] H. Li, D. G. Ouzounov, and F. W. Wise, "Starting dynamics of dissipative-soliton fiber laser," *Opt. Lett.*, vol. 35, pp. 2403–2405, 2010.
[224] L. Zinkiewicz, F. Ozimek, and P. Wasylczyk, "Witnessing the pulse birth-transient dynamics in a passively mode-locked femtosecond laser," *Laser Phys. Lett.*, vol. 10, p. 125003, 2013.
[225] X. Liu, "Soliton formation and evolution in passively-mode-locked lasers with ultralong anomalous-dispersion fibers," *Phys. Rev. A*, vol. 84: 023835, 2011. https://doi.org/10.1103/physreva.84.023835.
[226] X. Liu, "Dynamic evolution of temporal dissipative-soliton molecules in large normal path-averaged dispersion fiber lasers," *Phys. Rev. A*, vol. 82: 063834, 2010. https://doi.org/10.1103/physreva.82.063834.
[227] Y. Cui and X. Liu, "Revelation of the birth and extinction dynamics of solitons in SWNT-mode-locked fiber lasers," *Photonics Res.*, vol. 7, pp. 423–430, 2019.
[228] X. Wei, B. Li, Y. Yu, C. Zhang, K. K. Tsia, and K. K. Y. Wong, "Unveiling multi-scale laser dynamics through time-stretch and time-lens spectroscopies," *Opt. Express*, vol. 25, pp. 29098–29120, 2017.
[229] P. Ryczkowski, M. Närhi, C. Billet, J. M. Merolla, G. Genty, and J. M. Dudley, "Real-time full-field characterization of transient dissipative soliton dynamics in a mode-locked laser," *Nat. Photonics*, vol. 12, pp. 221–227, 2018.
[230] S. Sun, Z. Lin, W. Li, N. Zhu, M. Li, "Time-stretch probing of ultra-fast soliton dynamics related to Q-switched instabilities in mode-locked fiber laser," *Opt. Express*, vol. 26, p. 20888, 2018.
[231] R. Dunsmuir, "Theory of relaxation oscillations in optical masers," *J. Electron. Control*, vol. 10, pp. 453–458, 1961.
[232] H. -J. Chen, M. Liu, J. Yao, et al., "Buildup dynamics of dissipative soliton in an ultrafast fiber laser with net-normal dispersion," *Opt. Express*, vol. 26, pp. 2972–2982, 2018.
[233] H. J. Chen, M. Liu, J. Yao, et al., "Soliton booting dynamics in an ultrafast anomalous dispersion fiber laser," *IEEE Photonics J.*, vol. 10, p. 1501809, 2018.

[234] I. Kudelin, S. Sugavanam, and M. Chernysheva, "Build-up dynamics in bidirectional soliton fibre laser," *Photonics Res.*, vol. 8, pp. 776–780, 2020.
[235] Y. Yu, C. Kong, B. Li, et al., "Behavioral similarity of dissipative solitons in an ultrafast fiber laser," *Opt. Lett.*, vol. 44, pp. 4813–4816, 2019.
[236] G. Herink, F. Kurtz, B. Jalali, D. R. Solli and C. Ropers, "Real-time spectral interferometry probes the internal dynamics of femtosecond soliton molecules," *Science*, vol. 356, pp. 50–54, 2017.
[237] J. Peng and H. Zeng, "Build-up of dissipative optical soliton molecules via diverse soliton interactions," *Laser Photonics Rev.*, vol. 12, p. 1800009, 2018.
[238] A. Haboucha, H. Leblond, M. Salhi, A. Komarov, and F. Sanchez, "Analysis of soliton pattern formation in passively mode-locked fiber lasers," *Phys. Rev. A*, vol. 78: 043806, 2008. https://doi.org/10.1103/physreva.78.043806.
[239] Y. Meng, S. Zhang, X. Li, H. Li, J. Du, and Y. Hao, "Multiple-soliton dynamic patterns in a graphene mode-locked fiber laser," *Opt. Express*, vol. 20, pp. 6685–6692, 2012.
[240] V. Roy, M. Olivier, F. Babin, and M. Piché, "Dynamics of periodic pulse collisions in a strongly dissipative-dispersive system," *Phys. Rev. Lett.*, vol. 94, p. 203903, 2005.
[241] K. Krupa, K. Nithyanandan, U. Andral, P. Tchofo-Dinda, and P. Grelu, "Real-time observation of internal motion within ultrafast dissipative optical soliton molecules," *Phys. Rev. Lett.*, vol. 118, p. 243901, 2017.
[242] M. Liu, H. Li, A. P. Luo, H. Cui, W. C. Xu, and Z. C. Luo, "Real-time visualization of soliton molecules with evolving behavior in an ultrafast fiber laser," *J. Opt.*, vol. 20: 034010, 2018. https://doi.org/10.1088/2040-8986/aaabde.
[243] R. Xia, Y. Luo, P. Ping Shum, et al., "Experimental observation of shaking soliton molecules in a dispersion-managed fiber laser," *Opt. Lett.*, vol. 45, pp. 1551–1554, 2020.
[244] J. Peng, S. Boscolo, Z. Zhao, and H. Zeng, "Breathing dissipative solitons in mode-locked fiber lasers," *Sci. Adv.*, vol. 5, p. eaax1110, 2019.
[245] I. Mozjerin, S. Ruschin, and A. A. Hardy, "Analysis of relaxation oscillations and gain switching of unidirectional erbium-doped waveguide ring lasers," *IEEE J. Quantum Electron.*, vol. 46, pp. 158–163, 2010.
[246] Z. Wang, Z. Wang, Y. Liu, et al., "Self-organized compound pattern and pulsation of dissipative solitons in a passively mode-locked fiber laser," *Opt. Lett.*, vol. 43, pp. 478–481, 2018.
[247] Y. Wang, S. Y. Set, and S. Yamashita, "Active mode-locking via pump modulation in a Tm-doped fiber laser," *APL Photonics*, vol. 1: 071303, 2016. https://doi.org/10.1063/1.4965249.
[248] Y. C. Lee, C. T. Tsai, Y. C. Chi, Y. H. Lin, and G. R. Lin, "Chirp manipulation of harmonically mode-locked weak-resonant-cavity colorless laser diode with external fiber ring," *IEEE J. Quantum Electron.*, vol. 51, p. 1300111, 2015.
[249] Q. Hao, Y. Wang, P. Luo, H. Hu, and H. Zeng, "Self-starting dropout-free harmonic mode-locked soliton fiber laser with a low timing jitter," *Opt. Lett.*, vol. 42, pp. 2330–2333, 2017.
[250] M. E. Fermann and J. D. Minelly, "Cladding-pumped passive harmonically mode-locked fiber laser," *Opt. Lett.*, vol. 21, pp. 970–972, 1996.
[251] E. Yoshida, Y. Kimura, and M. Nakazawa, "Laser diode-pumped femtosecond erbium-doped fiber laser with a sub-ring cavity for repetition rate control," *Appl. Phys. Lett.*, vol. 60, pp. 932–934, 1992.
[252] Y. Zhao, S. Min, H. Wang, and S. Fleming, "High-power figure-of-eight fiber laser with passive sub-ring loops for repetition rate control," *Opt. Express*, vol. 14, pp. 10475–10480, 2006.
[253] C. S. Jun, J. H. Im, S. H. Yoo, et al., "Low noise GHz passive harmonic mode-locking of soliton fiber laser using evanescent wave interaction with carbon nanotubes," *Opt. Express*, vol. 19, pp. 19775–19780, 2011.
[254] X. Wang, J. Peng, K. Huang, M. Yan, H. Zeng, "Experimental study on buildup dynamics of a harmonic mode-locking soliton fiber laser," *Opt. Express*, vol. 27, pp. 28808–28815, 2019.
[255] W. He, M. Pang, D. H. Yeh, J. Huang, C. R. Menyuk, and P. S. J. Russell, "Formation of optical supramolecular structures in a fibre laser by tailoring long-range soliton interactions," *Nat. Commun.*, vol. 10, pp. 1–9, 2019.
[256] J. N. Kutz, B. C. Collings, K. Bergman, and W. H. Knox, "Stabilized pulse spacing in soliton lasers due to gain depletion and recovery," *IEEE J. Quantum Electron.*, vol. 34, pp. 1749–1757, 1998.
[257] D. A. Korobko, O. G. Okhotnikov, and I. O. Zolotovskii, "Long-range soliton interactions through gain-absorption depletion and recovery," *Opt. Lett.*, vol. 40, pp. 2862–2865, 2015.
[258] E. M. Dianov, A. V. Luchnikov, A. N. Pilipetskii, and A. N. Starodumov, "Electrostriction mechanism of soliton interaction in optical fibers," *Opt. Lett.*, vol. 15, pp. 314–316, 1990.
[259] A. B. Grudinin and S. Gray, "Passive harmonic mode locking in soliton fiber lasers," *J. Opt. Soc. Am. B.*, vol. 14, pp. 144–154, 1997.
[260] Y. Yu, B. Li, X. Wei, Y. Xu, K. K. M. Tsia, and K. K. Y. Wong, "Spectral-temporal dynamics of multipulse mode-locking," *Appl. Phys. Lett.*, vol. 110, p. 201107, 2017.
[261] X. Liu, "Interaction and motion of solitons in passively-mode-locked fiber lasers," *Phys. Rev. A*, vol. 84: 053828, 2011. https://doi.org/10.1103/physreva.84.053828.
[262] X. Liu, "Hysteresis phenomena and multipulse formation of a dissipative system in a passively mode-locked fiber laser," *Phys. Rev. A*, vol. 81: 023811, 2010. https://doi.org/10.1103/physreva.81.023811.
[263] D. Y. Tang, L. M. Zhao, B. Zhao, and A. Q. Liu, "Mechanism of multisoliton formation and soliton energy quantization in passively mode-locked fiber lasers," *Phys. Rev. A*, vol. 72: 043816, 2005. https://doi.org/10.1103/physreva.72.043816.
[264] F. X. Kärtner, J. Aus Der Au, and U. Keller, "Mode-locking with slow and fast saturable absorbers – what's the difference?," *IEEE J. Sel. Top Quantum Electron.*, vol. 4, pp. 159–168, 1998.
[265] A. Komarov, H Leblond, and F. Sanche, "Multistability and hysteresis phenomena in passively mode-locked fiber lasers," *Phys. Rev. A*, vol. 71: 053809, 2005. https://doi.org/10.1103/physreva.71.053809.
[266] S. -S. Xu, M. Liu, Z. -W. Wei, A. Luo, W. -C. Xu, and Z. -C. Luo, "Multi-pulse dynamics in a Mamyshev oscillator," *Opt. Lett.*, vol. 45, pp. 2620–2623, 2020.
[267] Y. Wei, B. Li, X. Wei, Y. Yu, and K. K. Y. Wong, "Ultrafast spectral dynamics of dual-color-soliton intracavity collision in a mode-locked fiber laser," *Appl. Phys. Lett.*, vol. 112: 081104, 2018. https://doi.org/10.1063/1.5020821.
[268] G. Wang, G. Chen, W. Li, C. Zeng, and H. Yang, "Decaying evolution dynamics of double-pulse mode-locking," *Photonics Res.*, vol. 6, pp. 825–829, 2018.

[269] X. Liu, X. Han, and Y. Zhang. *Observation of Multi-soliton Asynchronous Buildup Dynamics in all-PM Mode-locked Lasers*. arXiv:190502333, 2019.
[270] J. Zeng and M. Y. Sander, "Real-time transition dynamics between multi-pulsing states in a mode-locked fiber laser," *Opt. Lett.*, vol. 45, pp. 5–8, 2020.
[271] J. M. Soto-Crespo, N. Akhmediev, and A. Ankiewicz, "Pulsating, creeping, and erupting solitons in dissipative systems," *Phys. Rev. Lett.*, vol. 85, pp. 2937–2940, 2000.
[272] N. Akhmediev, J. M. Soto-Crespo, and G. Town, "Pulsating solitons, chaotic solitons, period doubling, and pulse coexistence in mode-locked lasers: complex Ginzburg-Landau equation approach," *Phys. Rev. E*, vol. 63: 056602, 2001. https://doi.org/10.1103/physreve.63.056602.
[273] J. M. Soto-Crespo, M. Grapinet, P. Grelu, and N. Akhmediev, "Bifurcations and multiple-period soliton pulsations in a passively mode-locked fiber laser," *Phys. Rev. E*, vol. 70: 066612, 2004. https://doi.org/10.1103/physreve.70.066612.
[274] Z. W. Wei, M. Liu, S. X. Ming, A. P. Luo, W. C. Xu, and Z. C. Luo, "Pulsating soliton with chaotic behavior in a fiber laser," *Opt. Lett.*, vol. 43, pp. 5965–5968, 2018.
[275] Y. Du, Z. Xu, and X. Shu, "Spatio-spectral dynamics of the pulsating dissipative solitons in a normal-dispersion fiber laser," *Opt. Lett.*, vol. 43, pp. 3602–3605, 2018.
[276] M. Liu, Z. W. Wei, H. Li, et al., "Visualizing the "invisible" soliton pulsation in an ultrafast laser," *Laser Photonics Rev.*, vol. 14, p. 1900317, 2020.
[277] C. R. Menyuk, "Stability of solitons in birefringent optical fibers I: equal propagation amplitudes," *Opt. Lett.*, vol. 12, pp. 614–616, 1987.
[278] C. R. Menyuk, "Stability of solitons in birefringent optical fibers. II. Arbitrary amplitudes," *J. Opt. Soc. Am. B.*, vol. 5, pp. 392–401, 1988.
[279] D. Mao, X. Liu, and H. Lu, "Observation of pulse trapping in a near-zero dispersion regime," *Opt. Lett.*, vol. 37, pp. 2619–2621, 1988.
[280] Y. Song, X. Shi, C. Wu, D. Tang, and H Zhang, "Recent progress of study on optical solitons in fiber lasers," *Appl. Phys. Rev.*, vol. 6: 021313, 2019. https://doi.org/10.1063/1.5091811.
[281] D. Y. Tang, H. Zhang, L. M. Zhao, and X. Wu, "Observation of high-order polarization-locked vector solitons in a fiber laser," *Phys. Rev. Lett.*, vol. 101, p. 153904, 2008.
[282] K. Krupa, K. Nithyanandan, and P. Grelu, "Vector dynamics of incoherent dissipative optical solitons," *Optica*, vol. 4, pp. 1239–1244, 2017.
[283] Y. Cui, Y. Zhang, Y Xiang, Y. Song, and X. Liu. *XPM-forced Frequency-Oscillating Soliton in Mode-locked Fiber Laser*. arXiv:191009225, 2019.
[284] Y. Cao, L. Gao, Y. Li, et al., "Polarization-dependent pulse dynamics of mode-locked fiber laser with near-zero net dispersion," *Appl. Phys. Express*, vol. 12, p. 112001, 2019.
[285] S. C. V. Latas and M. F. S. Ferreira, "Soliton explosion control by higher-order effects," *Opt. Lett.*, vol. 35, pp. 1771–1773, 2010.
[286] S. T. Cundiff, J. M. Soto-Crespo, and N. Akhmediev, "Experimental evidence for soliton explosions," *Phys. Rev. Lett.*, vol. 88: 073903, 2002. https://doi.org/10.1103/physrevlett.88.073903.
[287] A. F. J. Runge, N. G. R. Broderick, and M. Erkintalo, "Observation of soliton explosions in a passively mode-locked fiber laser," *Optica*, vol. 2, pp. 36–39, 2015.
[288] A. F. J. Runge, N. G. R. Broderick, and M. Erkintalo, "Dynamics of soliton explosions in passively mode-locked fiber lasers," *J. Opt. Soc. Am. B.*, vol. 33, pp. 46–53, 2016.
[289] J. Peng and H. Zeng, "Experimental observations of breathing dissipative soliton explosions," *Phys. Rev. Appl.*, vol. 12: 034052, 2019. https://doi.org/10.1103/physrevapplied.12.034052.
[290] Y. Yu, Z. -C. Luo, J. Kang, and K. K. Y. Wong, "Mutually ignited soliton explosions in a fiber laser," *Opt. Lett.*, vol. 43, pp. 4132–4135, 2018.
[291] B. H. Kolner and M. Nazarathy, "Temporal imaging with a time lens," *Opt. Lett.*, vol. 14, pp. 630–632, 1989.
[292] C. Zhang, J. Xu, P. C. Chui, and K. K. Y. Wong, "Parametric spectro-temporal analyzer (PASTA) for real-time optical spectrum observation," *Sci. Rep.*, vol. 3, p. 2064, 2013.
[293] P. Suret, R. El Koussaifi, A. Tikan, et al., "Single-shot observation of optical rogue waves in integrable turbulence using time microscopy," *Nat. Commun.*, vol. 7, p. 13136, 2016.
[294] M. Närhi, B. Wetzel, C. Billet, et al., "Real-time measurements of spontaneous breathers and rogue wave events in optical fibre modulation instability," *Nat. Commun.*, vol. 7, p. 13675, 2016.
[295] F. Copie, M. Conforti, A. Kudlinski, S. Trillo, and A. Mussot, "Dynamics of Turing and Faraday instabilities in a longitudinally modulated fiber-ring cavity," *Opt. Lett.*, vol. 42, pp. 435–438, 2017.
[296] G. Pu, L. Yi, L. Zhang, C. Luo, Z. Li, and W. Hu, "Intelligent control of mode-locked femtosecond pulses by time-stretch-assisted real-time spectral analysis," *Light Sci. Appl.*, vol. 9, p. 13, 2020.